

Master's thesis

Chemical Engineering and Biotechnology

2022

Laura Jokinen

OPTIMISING FLOCCULATION  
AND CELL SEPARATION OF  
FERMENTATION BROTH WITH  
*IN-SITU* PARTICLE SIZE  
ANALYSIS

Laura Jokinen

# OPTIMISING FLOCCULATION AND CELL SEPARATION OF FERMENTATION BROTH WITH IN-SITU PARTICLE SIZE ANALYSIS

The aim of this study was to examine whether the flocculation and cell separation of fermentation broth could be reliably optimised *in-situ* with particle size analyser based on particle vision and measurement technique. Flocculation is part of a two-step coagulation-flocculation process in which particles are collided together to form aggregates and eventually macroflocs. The higher weight of the particles increases the efficiency of sedimentation and separation unit operations.

The aim of the optimisation was to achieve the best possible filtration flux as well as filtrate quality. Filtrate quality was determined with turbidity meter. The lower the turbidity the higher the quality since low turbidity indicates that more particles have been part of microfloc formation. More high-quality filtrate can lead to more efficient downstream process steps which comes after cell separation.

Four fungal and *Bacillus* processes were selected for this purpose. Four flocculant dosages were tested with laboratory scale and/or pilot scale material along with reference without flocculation. Particle size analysis measurements were conducted with Easy Viewer 100 -probe and iC Vision software by Mettler-Toledo. Every dosage was cell separated after the measurement with micro scale pressure filter. Cell separation fluxes and filtrate quality were compared with particle size distribution curves to determine the optimal dosage.

Promising results were obtained from the *Bacillus* processes. The cell separation fluxes multiplied with the optimal flocculant dosage and the change in particles could be observed from the pictures taken by the probe and peak of chord length distribution moved towards larger particles and the total number of particles decreased.

Flocculation of fungal processes led only to minor shifts in chord length distributions. The changes were also difficult to interpret from the curves. No floc formation could either be seen in the pictures. The optimal dosage of flocculant could nevertheless be determined based on cell separation fluxes and filtrate quality in combination with the chord length distributions.

Based on the results, particle vision and measurement-based particle size analysis could be used for optimising flocculation for *Bacillus* broths, but more data should be gathered to be able to rely solely on the particle size analysis. For fungal broths other particle size analysis technique could be tested as an option and continue with cell separation tests for accurate flocculant dosing.

## KEYWORDS:

Flocculation, coagulation, cell separation, chord length distribution, particle vision and measurement

Laura Jokinen

# FLOKKULOINNIN JA SOLUEROTUKSEN OPTIMOINTI IN-SITU PARTIKKELIKOKOANALYSILLÄ

Tämän tutkimuksen tavoitteena oli selvittää, voidaanko fermentointiliemen flokkulointia ja soluerotusta optimoida luotettavasti *in-situ* kuva-analyysiin perustuvalla partikkelikokoanalyysaattorilla. Flokkulointi on osa kaksivaiheista koagulointi-flokkulointiprosessia, jossa suspensioissa olevat hiukkaset törmäävät toisiinsa muodostaen aggregaatteja ja makroflokkeja. Hiukkasten suurempi koko tehostaa sedimentaatio- ja erotusprosesseja.

Optimoinnin tavoitteena oli saavuttaa mahdollisimman hyvä suodatusnopeus sekä suodoksen laatu. Työssä suodoksen laatu määritettiin sameusmittauksilla. Mitä kirkkaampi suodos sitä parempi sen laatu on. Suodoksen alhaisempi sameus indikoi, että suurempi osa partikkeleista on ollut mukana makroflokkien muodostamisessa. Kirkkaampi suodos johtaa useimmiten myös tehokkaampiin soluerotuksen jälkeisiin jälkikäsittelyvaiheisiin.

Tätä tarkoitusta varten valittiin neljä home- ja *Bacillus*-prosessia. Neljää eri flokkulanttiannostusta testattiin laboratorio- ja/tai pilottimitassa tuotetulla materiaalilla. Soluerotus ilman flokkulointia toimi kaikissa kokeissa referenssinä. Partikkelikokoanalyysi suoritettiin Easy Viewer 100 -anturilla ja Mettler-Toledon iC Vision -ohjelmistolla. Partikkelikokoanalyysin jälkeen jokaiselle kokeelle tehtiin soluerotus laboratoriomittakaavan painesuodattimella. Suodatusnopeutta ja suodoksen laatua verrattiin partikkelikokoajakäyriin optimaalisen annostuksen määrittämiseksi.

*Bacillus*-prosesseista saatiin lupaavia tuloksia. Soluerotuksen suodatusnopeus moninkertaistui optimaalisella flokkulantin annostuksella ja partikkelikoon muutos oli havaittavissa anturin ottamista kuvista sekä partikkelikokoajakäyrien huippu siirtyi kohti suurempia hiukkasia. Samalla hiukkasten kokonaismäärä pieneni.

Homeprosessien flokkulointi johti vain vähäisiin muutoksiin hiukkaskokoajakäyrimissä. Muutoksia oli myös vaikea tulkita käyristä. Kuvissa ei myöskään näkynyt flokkien muodostumista. Flokkulantin optimaalinen annostus voitiin kuitenkin määrittää soluerotuksen suodatusnopeuden ja suodoksen laadun perusteella yhdessä partikkelikokoajakäyrien kanssa.

Tulosten perusteella kuva-analyysiin perustuvaa partikkelikokoanalyysiä voidaan hyödyntää *Bacillus*-liemien flokkuloinnin optimointiin, mutta kokeita tulisi tehdä lisää, jotta voidaan luottaa pelkästään partikkelikokoanalyysiin. Homeliemille voi olla hyödyllistä testata vaihtoehtoisia tekniikkoa partikkelikokoanalyysiin suorittamiseen ja jatkaa soluerotuskokeita flokkulanttien annostuksen määrittämiseksi.

## ASIASANAT:

Flokkulointi, koagulointi, soluerotus, partikkelikoko, partikkelikokoanalyysi

# CONTENT

<b>LIST OF ABBREVIATIONS</b>	<b>9</b>
<b>1 INTRODUCTION</b>	<b>8</b>
<b>2 COAGULATION-FLOCCULATION PROCESS</b>	<b>10</b>
2.1 Principles in colloidal system and coagulation-flocculation process	10
2.2 Coagulation and flocculation agents	12
2.2.1 Coagulants	12
2.2.2 Flocculants	13
2.2.3 Alternative chemicals and aids	14
2.3 Applications	15
2.3.1 Wastewater treatment	15
2.3.2 Pulp and paper industry	16
2.3.3 Metal mining	16
2.3.4 Biomass harvesting and separation	17
<b>3 COAGULATION AND FLOCCULATION PROCESS CONTROL AND METHODS FOR OPTIMISATION</b>	<b>18</b>
3.1 Coagulation and flocculation process optimisation	18
3.2 Parameters used in process control	18
3.2.1 Chemical type and concentration	18
3.2.2 Mixing	19
3.2.3 pH	20
3.2.4 Turbidity	20
3.2.5 Temperature	21
3.3 Methods for optimisation	21
3.3.1 Jar testing	21
3.3.2 Conductivity and ionic strength	22
3.3.3 Zeta potential	23
3.3.4 Turbidity measurement	23
3.3.5 Optical density	24
3.3.6 Focused beam reflectance measurement	25
3.3.7 Particle vision and measurement	27

<b>4 CELL SEPARATION OF FERMENTATION BROTH</b>	<b>29</b>
4.1 Solid-liquid separation by sedimentation and centrifugation	29
4.1.1 Principle	29
4.1.2 Sedimentation and centrifugation techniques	30
4.2 Solid-liquid filtration	32
4.2.1 Principle	32
4.2.2 Filter media	34
4.2.3 Filter aids	35
4.2.4 Principles of dead-end filtration in cell separation	36
4.2.5 Principles of crossflow filtration in cell separation	39
<b>5 MATERIALS AND METHODS</b>	<b>41</b>
5.1 Background	41
5.2 Fungal and <i>Bacillus</i> fermentation processes	41
5.3 Equipment	42
5.3.1 Particle size analyser	42
5.3.2 Lab scale pressure filter for cell separation	43
5.4 Experimental set-up	44
<b>6 RESULTS</b>	<b>46</b>
6.1 Fungal processes	46
6.1.1 Optimising flocculation and cell separation of A1	46
6.1.2 Optimising flocculation and cell separation of A2	48
6.1.3 Optimising flocculation and cell separation of B1	50
6.1.4 Optimising flocculation and cell separation of B2	52
6.2 <i>Bacillus</i> processes	54
6.2.1 Optimising flocculation and cell separation of C1	54
6.2.2 Optimising flocculation and cell separation of C2	58
6.2.3 Optimising flocculation and cell separation of D1	61
<b>7 CONCLUSIONS</b>	<b>65</b>
<b>REFERENCES</b>	<b>68</b>

# APPENDICES

## Appendix 1. iC Vision microscopic captures and chord length distributions

### FIGURES

Figure 1. Effect of flocculant type. (Mettler-Toledo, 2021)	19
Figure 2. Effect of shear forces on three floc types. (Aldajani & al., 2021)	20
Figure 3. Change of ionic strength $\Delta\sigma$ and the relaxation time ( $\tau$ ) as a function of the coagulant concentration. With the optimal dosage, the lowest level of ionic strength and the highest relaxation time is achieved. (Mortadi & al., 2020)	23
Figure 4. In dead-end filtration solids build up thickening the cake which leads to decrease in permeate flux. (Harrison & al., 2015, p. 143)	38
Figure 5. A Constant permeate flux in steady state cross-flow filtration. (Harrison & al., 2015, p. 143)	39
Figure 6. Workflow in the experimental part. Every measurement and filtration were performed separately.	45
Figure 7. Relative fluxes for test A1.	46
Figure 8. Turbidity of A1 filtrates.	47
Figure 9. A1 with flocculant dosage 2. Number of count increases but no difference can be seen in chord length.	47
Figure 10. Relative cell separation fluxes for A2.	49
Figure 11. Turbidity of A2 filtrates.	49
Figure 12. A2 with flocculant dosage 3. Number of counts increased but no difference can be seen in chord lengths.	50
Figure 13. Relative cell separation fluxes for B1.	51
Figure 14. Turbidity of B1 filtrates.	51
Figure 15. B1 with flocculant dosage 3. Number of counts decreased slightly, and a difference can be seen between rapid and slow mixing phases in particle counts larger than 100 $\mu\text{m}$ .	52
Figure 16. Relative cell separation fluxes for B2.	53
Figure 17. Turbidity of B2 filtrates.	53
Figure 18. B2 with flocculant dosage 3. Number of counts decreased slightly. Only minor difference can be seen between rapid and slow mixing phases in particle counts in $>100 \mu\text{m}$ and $<10 \mu\text{m}$ .	54
Figure 19. Relative cell separation fluxes for C1.	55
Figure 20. Turbidity of C1 filtrates.	55
Figure 21. C1 with flocculant dosage 3. The peak shifted towards larger particles after flocculation.	56
Figure 22. Relative cell separation fluxes for C2.	58
Figure 23. Turbidity of C2 filtrates.	59
Figure 24. C2 with flocculant dosage 2. The peak shifted towards larger particles after flocculation.	59
Figure 25. Relative cell separation fluxes for D1.	62
Figure 26. Turbidity of D1 filtrates.	62
Figure 27. D1 with flocculant dosage 1. Number of small particles decreased, and large ones increased.	63

## EQUATIONS

Equation 1. Flocculation efficiency calculated with turbidity measurements. NTU refers to the nephelometric turbidity unit which is measured with turbidity meter. Turbidity of a control measurement in the equation is turbidity of the supernatant without flocculation after settling. (Ajao & al., 2021)	24
Equation 2. Flocculation efficiency calculated with optical density measurements. $OD_t$ is the density of supernatant after flocculation and settling and $OD_{t0}$ density of supernatant after settling buy without flocculation. (Hadiyanto & al., 2021)	25
Equation 3. Centrifugal acceleration. (Harrison & al., 2015, p. 180)	30
Equation 4. Darcy's law describes flow of the liquid through the cake. (Harrison & al., 2015, p. 144)	38
Equation 5. The rate of convective mass transfer of solute toward the membrane surface at steady state of crossflow filtration. (Harrison & al., 2015, p. 148)	39

## PICTURES

Picture 1. Three principles of coagulation: 1a. Repulsive forces prevents aggregation, 1b. Coagulant dispersion and 1c. Microfloc formation. (Mettler-Toledo, 2021)	11
Picture 2. 2a. Formation of macroflocs: 2b. Loosely packed flocs. (Mettler-Toledo, 2021)	12
Picture 3. Jar testing equipment for testing coagulation-flocculation process in wastewater treatment plant. (Ali & al., 2009)	21
Picture 4. Simple filtration system for jar testing. (Bratby, 2016, p. 366)	22
Picture 5. Schematic of a FBRM probe: solid-state laser light is focused to small area at a constant distance from the sapphire window. Particles that pass the window backscatter the laser light back to the probe and on to light detector through optical modules. (Kyodaab & al., 2019)	26
Picture 6. a) Sematic of front-end illuminating PVM probe. b) Layout of the probe. (Chianese, A. & al., 2012, p. 41)	27
Picture 7. High quality image of Ammonium Sulphate taken by PVM where light source and detector are separated. (Chianese, A. & al., 2012, p. 42)	28
Picture 8. Schematic of tubular centrifuge. (Harrison & al., 2015, p. 187)	31
Picture 9. Schematic of disc centrifuge and the liquid flow. (Harrison & al., 2015, p. 187-190)	32
Picture 10. Direct interception. Small particles are removed if they hit opening simultaneously. (Perlmutter, 2015, p. 7)	33
Picture 11. Dead-end filtration (a) compared to crossflow filtration (b). (Harrison & al., 2015, p. 143)	34
Picture 12. Close-up to synthetic plain wave with large openings. (Perlmutter, 2015, p. 11)	34
Picture 13. Structure of diatomite particle. (Sarasti, 2017, p. 12)	36
Picture 14. Easy Viewer 100 probe. Sapphire window is located in the tip of the probe. (Mettler-Toledo, 2021)	42
Picture 15. Microscopic picture of fermentation broth in iCVision software taken by the Easy Viewer 100 probe.	43

Picture 16. Capture from iC Vision before flocculation of A1.	48
Picture 17. Capture from iC Vision after flocculant dosage 2 and slow mixing (A1). No clear visual flocculation.	48
Picture 18. Microscopic picture of C1 before flocculation.	57
Picture 19. C1 after flocculation with dosage 3. The flocs are clearly visible.	57
Picture 20. Microscopic picture of C2 before flocculation. Halos are visible in the corners of the picture.	60
Picture 21. Microscopic picture of C2 after flocculant dosage 2. The flocs are clearly visible.	61
Picture 22. Microscopic picture of D1 before flocculation.	63
Picture 23. Microscopic picture of D1 after flocculation with dosage 1. The flocs are small but still visible to eye.	64

## TABLES

Table 1. Examples of coagulant and flocculant agents. (Ajao & al., 2020; Dayarathne & al., 2021; Kemira Oyj, 2021; Pandey, 2014)	15
Table 2. Examples of dead-end filtration systems. (Perlmutter, 2015)	37
Table 3. Selected processes and coding.	41
Table 4. Main settings of the Easy Viewer 100 probe and iC Vision software for all experiments.	44
Table 5. Filtration data for test series A1.	46
Table 6. Filtration data for test series A2.	49
Table 7. Filtration data for test series B1.	51
Table 8. Filtration data for test series B2.	53
Table 9. Filtration data for test series C1.	55
Table 10. Filtration data for test series C2.	58
Table 11. Filtration data for test series D1.	61

## LIST OF ABBREVIATIONS

CLD	Chord length distribution
DSP	Downstream process
DM	Dry matter, total weight - moisture content
EPS	Microbial extracellular polymeric substance
FBRM	Focused Beam Reflectance Measurement
FE	Flocculation efficiency
HMWP	High molecular weight polymer (> 10 000 kDA)
HPAM	Hydrolyzed polyacrylamide
<i>In-situ</i>	Measuring straight from process without sampling
NTU	Nephelometric turbidity unit
OD <sub>680</sub>	Optical density at 680 nm
PSA	Particle size analysis
P&P	Pulp and paper
PVM	Particle vision and measurement

# 1 INTRODUCTION

Cell separation of fermentation broth is a unit operation where microbial cells and possible insoluble medium components are separated from a liquid phase. The liquid phase contains the desired product, for instance a protein. Microbial cells can also keep the product inside the cell. Then, cell lysis must be performed before the cell separation step. This process step is known to consume resources and substantial product losses are possible.

With optimal flocculation prior cell separation, more efficient cell separation can be achieved with low product losses and shortened process time. Underdosing flocculant agent will make the cell separation slower. Overdosing of the flocculant agent can lead to difficulties in following process steps in the downstream process such as concentration and purification due to flow through of the flocculant agent and other particles and will increase raw material costs. Optimal dosing can also increase product quality since by-products are removed from the liquid.

The aim of this thesis was to examine whether the flocculation and cell separation of fermentation broth could be reliably optimised with *in-situ* particle size analysis. For this purpose, suitable fungal and *Bacillus* process were selected for optimisation. Fermentation process of these strains had been finalised, but downstream process is still under development. Several flocculation concentrations were tested in each process and laboratory scale cell separation was performed to all. Particle size distribution and microscopic pictures were taken from every experiment prior cell separation with the *in-situ* particle size analyser which is based on particle vision and measurement technique. Small feasibility study was conducted earlier for flocculation monitoring with fungal broth using focused beam reflectance measurement-based particle size analyser. The study gave promising results.

There are multiple technologies to study particle size, shape, and distribution but which are developed for sediment and soil samples and thus are not applicable in bioprocessing and in solid-liquid samples. This thesis concentrates on a technique which can be used in bioprocessing. The particle size analyser used in this study has been mainly used to examine particles and droplets in suspensions and emulsions and tracking process changes is crystallization and precipitation. Aim is to verify whether it

can reliably also be used in monitoring and analysing flocculation in fungal and *Bacillus* broths.

Cell separation was done to every measurement and results were compared with particle distribution curves and microscopic pictures. The success of the flocculation and cell separation was evaluated based on filtration flux and filtrate quality. Filtrate quality is determined with turbidity meter. The lower the turbidity the higher quality.

Particle size analysis could be part of a routine process development in flocculation and cell separation phase if it is proven to be feasible. The number of laboratory scale filtrations tests that require fair number of resources could then be reduced and make use of elsewhere.

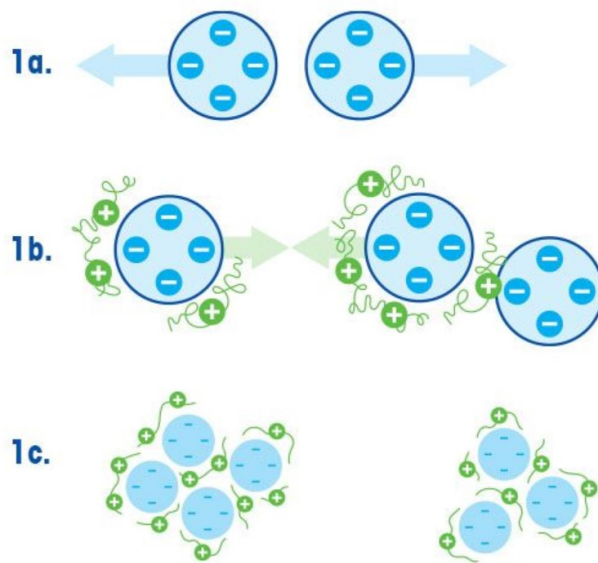
This thesis is divided into theory and experimental parts. The principle of coagulation-flocculation process, choices for flocculation process control and cell separation techniques used in the industry are explained in the theory part. Methods and materials, results and conclusions are presented in the experimental part.

## 2 COAGULATION-FLOCCULATION PROCESS

### 2.1 Principles in colloidal system and coagulation-flocculation process

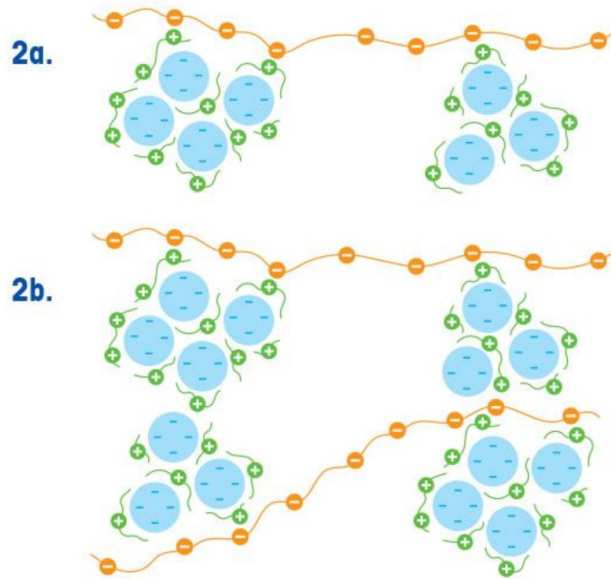
Majority of bioparticles suspended in aqueous solutions are negatively charged. Repulsive force prevents them from forming larger particles through aggregation. Coagulation-flocculation is a two-step process to increase particle size, and which is commonly divided into four parts: charge shielding, the neutralization of the charges, formation of electrostatic batches and formation of bridges between particles. Coagulation-flocculation process is performed prior filtration or other liquid-solid separation unit operations. (Mortadi & al., 2020; Sustainable Sanitation and Water Management, 2021)

A suspension in which particles do not aggregate is called a stable colloidal suspension. The transition to unstable non-colloidal suspension requires the reduction of the surface charges of the particles. Charge shielding and neutralization and the formation of the electrostatic batches are part of coagulation. In coagulation step positively charged coagulant agent is added to the solution. Coagulant chemical will absorb the negatively charged particles as illustrated in Picture 1. This neutralises the negative charges of the colloidal particles. After neutralisation small particles can form microflocs by electrostatic forces. In practise positively charged coagulant attaches to negatively charged particle. Sufficient mixing is needed when adding the coagulant agent to properly disperse it to the solution and to promote particle collision in microfloc formation. Insufficient mixing will lead to incomplete coagulation. Coagulation step usually lasts from 1 to 3 minutes. (Tadros, 2017; SSWM, 2021)



Picture 1. Three principles of coagulation: 1a. Repulsive forces prevents aggregation, 1b. Coagulant dispersion and 1c. Microfloc formation. (Mettler-Toledo, 2021)

In flocculation step suspension and the micro flocs are gently mixed to bring the particles into collisions. This causes even more collisions and bridges form between particles and leads to formation of macroflocs. Flocculants which are mainly high molecular weight polymers (HMWP) can be added at this stage to induce the bridging. Bridging flocculation occurs because parts of the polymer chain adsorb simultaneously on different particles and links them together as seen in Picture 2. Effective bridging flocculation requires that the polymer extends far enough from the particle surface to attach to other particles and that there is sufficient free surface available for adsorption in the particles. When excess polymer is added, the particles can be saturated with the polymer and the particles cannot be linked together. Bridging will strengthen the flocs and add weight. When particles are closer together, Van Der Waals attraction force begin to affect. As the flocs increase in size the van der Waals force also increase. Van der Waals contact distance is a distance where attraction forces overcome repulsive forces and particles can aggregate more efficiency. It reduces the energy needed for flocculation and loosely packed flocs can form which should become visible to eye. The Higher weight increases the efficiency of sedimentation and separation processes (Dayarathne & al., 2021; SSWM, 2021)



Picture 2. 2a. Formation of macroflocs: 2b. Loosely packed flocs. (Mettler-Toledo, 2021)

## 2.2 Coagulation and flocculation agents

### 2.2.1 Coagulants

Coagulant can be applied with or without flocculant and vice versa but usually most efficient result is obtained using both. Coagulants and flocculants can be both be cationic and anionic depending on the application. (Aldajani & al., 2021; Dayarathne & al., 2021)

Coagulant chemicals can be divided into inorganic salts and inorganic polymeric coagulants. They are widely used due to their low cost. With inorganic coagulants strong micro flocs are achieved which are relatively resistant to shear forces. They are sensitive to pH and might therefore lack efficiency in some applications. Coagulants can form hazardous end products and are not biodegradable. (Aldajani & al., 2021; Dayarathne & al., 2021)

Inorganic salts used as coagulants are usually aluminium or iron salts such as Aluminium Chlorohydrate  $\text{Al}_2\text{ClH}_7\text{O}_6$  and Ferric Sulphate  $\text{Fe}_2(\text{SO}_4)_3$ . Titanium and zinc salt coagulants also exists but are less used due to higher price and toxicity even though they are more efficient in charge neutralisation and can form larger size flocs. Iron salts can neutralize charges particularly efficiently. (Dayarathne & al., 2021; Kemira Oyj, 2021)

Polymeric coagulants are inorganic polymers which have electrical charges and are also called as polyelectrolytes. Polyelectrolytes consist of repeats of metallic salts and therefore have higher charges compared to metallic salts. High charge is more likely to interact with particles in the suspension. (Dayarathne & al., 2021)

### 2.2.2 Flocculants

Flocculants act by forming interparticle molecular bridges between unstable colloidal particles, in which case the flocculants are usually polymers or smaller oligomers. The most effective flocculants are typically polyelectrolytes with an opposite charge to that of the particles. With oppositely charged polyelectrolytes adsorption is more likely to occur and the strong electrostatic attraction between the positive ionic groups of the polymer and the negative charged particle surface is being formed. Flocculants can also act by reducing the repulsive forces between the particles by reducing the strength of the electrostatic field. Flocculant agents are always water soluble. (Harrison & al., 2015; Tadros, 2017)

Flocculant agents can be divided into synthetic polymers and biopolymers. There are also flocculants combining organic polymers and inorganic salts (composite) and combinations of synthetic polymer and biopolymer. For example, synthetic acrylamide can be polymerized with biobased lignin to produce more effective flocculant for wastewater treatment. Polymers can form bridges between particles via different pathways. Ion binding can occur between cationic surfaces and anionic polymers when there are enough divalent ions present such as  $\text{Ca}^{2+}$ . Another pathway is through covalent bonds between the polymers H-atoms and more electronegative atoms or molecules. (Aldajani & al., 2021; Dayarathne & al., 2021)

Fossil based synthetic polymer flocculants such as polydiallyldimethylammonium chloride (shortened polyDADMAC), are non-biodegradable and, in many cases, highly toxic and carcinogenic. Molecular size varies between 1 and 20 million Daltons in synthetic polymer flocculants. Monomers which are degradation products of the synthetic polymers may also be toxic. This causes limitations at where synthetic polymers can be applied. The most used synthetic polymer is acrylamide. It is a white salt which can be both cationic and anionic. (Ajao & al., 2020; Aldajani & al., 2021)

Biopolymers lack the toxicity and are therefore widely used in food, medicine, and agricultural applications. The use of bio-based flocculants is increasing while new substances arise and comparable performance to synthetic ones is achieved. Bio-based polymers are typically dosed as mixtures containing different molecular weight versions of the same polymer. (Ajao & al., 2020; Aldajani & al., 2021)

### 2.2.3 Alternative chemicals and aids

Many conventional flocculant and coagulant agents have hazardous by-products, are acidic, metal salts and their ions are corrosive, and some are in high dosages risk to plant, animal, and human health. Storage and handling can also cause risk to humans and environment. Biggest challenges are nevertheless met in disposal of sludges, sediments, and the solid matter after coagulation-flocculation process and thus there is a growing demand in more environmentally friendly coagulant and flocculant agents. (Dayarathne & al., 2021)

Depending on the application, the solid matter is treated or disposed in different means due to chemical residues and end-products, but additional process steps might be needed which increases the cost of the production process. There are studies ongoing on several alternative chemicals and bio flocculants of which examples can be seen in Table 1. For instance, nanotubes, micro algae, and aluminium based hybrid coagulants have been tested in wastewater treatment with positive outcome. (Dayarathne & al., 2021)

Table 1. Examples of coagulant and flocculant agents. (Ajao & al., 2020; Dayarathne & al., 2021; Kemira Oyj, 2021; Pandey, 2014)

<b>Chemical group</b>	<b>Examples of substances</b>
Inorganic salts	Aluminium Chloride, Ferric Sulphate, Ferric Chloride, Zinc Sulphate, Aluminium Sulphate, Titanium Chloride
Polymeric salts	Polyaluminum Chloride, Polyaluminum Silica Sulphate, Polyferric chloride
Synthetic polymers	Polyacrylamide, polyamine, polyDADMAC, polymethacrylate
Biopolymers	Lignin, chitosan, starch, EPS, cellulose and cellulose derivatives, gelatines, galactomannans
Alternative chemicals	Carbon nanotubes, zirconium, pumice, crushed shells, sea bream scale, hibiscus, hybrids combining conventional and alternative chemicals, microalgae, <i>Aspergillus</i> sp.

Coagulant aids may have high impact on the coagulation process. Aids are used to decrease the needed chemical dosage which reduces the possibility of difficulties in following process steps caused by the high coagulant amounts. Aids may also be needed for forming bigger flocs. Activated silica and alginates are examples of coagulation aids. (Dayarathne & al., 2021)

## 2.3 Applications

### 2.3.1 Wastewater treatment

Flocculation processes have a wide range of applications in many industries such as wastewater treatment, pulp and paper, production of pharmaceuticals and mineral processing.

Coagulation and flocculation process is the most used method in wastewater treatment process due to its' effectiveness and low cost. Regulatory limits for tap water are high in regards of turbidity. Wastewater can be divided into industrial wastewater and domestic wastewater. Industrial wastewater consists of organic, inorganic, and metal particles. Settling of these particles is complicated and they have high surface charges. Natural

polymers have moderate efficiency in industrial wastewater flocculation. (Aldajani & al., 2021; Bratby, 2016)

Domestic wastewater treatment begins with coagulation-flocculation process and is followed by sedimentation. Coagulation-flocculation is important in the sediment removal but also in preventing membrane clogging in micro- and ultrafiltration stages. Aluminium sulphate is the most used coagulant in domestic wastewater treatment. It is manufactured from bauxite with sulfuric acid. (Bratby, 2016)

### 2.3.2 Pulp and paper industry

Cellulose fibre is one of the main ingredients in pulp and paper, but it also requires glue, impregnation, and fillers to achieve the required sheet properties for an acceptable paper product. Flocculation is the key processing step to combine fibres, fillers, and other additives in such a way that it dewateres quickly and can be produced in large quantity. More special uses of flocculation in the P&P industry are to remove toxic wood extractives, such as colloidal resin acids, residual suspended solids, and coloured substances in paper production. (Liu & al., 2011)

Acidified Aluminium Sulphate is widely used coagulant in the pulp and paper industry due to its' low pH range and low cost. (Liu & al., 2011)

### 2.3.3 Metal mining

In metal mining ore product streams often contain a wide range of different metals, which need to be separated in order to obtain pure products. This can be accomplished with precipitation of the individual metals. The formation of mineral or metal aggregates are promoted with flocculants. Flocculation ensures quick separation from the rest of the ore through sedimentation. Most common flocculation chemical in mining is hydrolysed polyacrylamides (HPAM) with varying anionic charge densities. HPAM develops the aggregates through polymer bridging. Segments of the HPAM attaches to different particles to bridge between them and forms large but porous and fragile flocs that settle rapidly. Flocculation with HPAM tends to need addition of coagulant agent prior flocculation. (Mettler-Toledo, 2021; Ramos & al., 2020)

#### 2.3.4 Biomass harvesting and separation

Coagulation-flocculation process is used in biopharma and other biotechnology segments to ease cell separation and to increase the product recovery. In biofuel production the aim is to increase the recovery of the biomass for example in microalgae harvesting by sedimentation, flotation, filtration, or centrifugation. (Pandey, 2014)

Flocculation is utilized in such conditions where cells and insoluble substances need to be separated prior filtration or settling. Mammalian cells are usually rather manageable in cell separations as their cell size is relatively larger compared to other cell types. Bacterial, microalgae and yeasts have much smaller cells but usually higher biomass and thus more laborious to harvest. The amount of biomass and small particles and the particle size can create small cell fragments which clog filters and slow down the separation rates. (Mettler-Toledo, 2021)

Coagulation-flocculation is used to decrease the amount of these small cell fragments and to aggregate small cells together. Larger cell pellets sediment faster and less clogging of filters is experienced. Also, by coagulant-flocculation the number of by-products can be decreased which increases the end product quality. Applying flocculation may lead to higher flux in filtration or settling speed in cost-effective way. (Pandey, 2014)

Industry's regulations impose restrictions on what coagulants or flocculation agents can be utilised in the biomass harvesting and cell separations especially in biopharma industry. The added coagulants and flocculant are expensive to remove afterwards from the products and thus it needs to be selected in such way that it does not impose issues later and overdosing needs to be avoided. (Pandey, 2014)

## **3 COAGULATION AND FLOCCULATION PROCESS CONTROL AND METHODS FOR OPTIMISATION**

### **3.1 Coagulation and flocculation process optimisation**

Process optimisation can be considered as continuous quality improvement. A process can be optimised only after understanding how to best control it. The right information is needed to achieve the correct method for control. To retrieve the correct information experiment needs to be planned in accurate way and the information achieved needs to be interpret and analysed correctly. (Evans, 2003)

An optimum dosage of flocculant is needed because at low concentrations there is insufficient amount of polymer present to provide adequate links and with larger amounts the surfaces of the particles can be covered with the polymer. In that case no bridging is possible since the surface is then only positively charged. With the optimal coagulation-flocculation dosage the following process step will be more efficient. (Dayarathne & al., 2021; Tadros, 2017)

There are multiple ways to monitor coagulation and flocculation processes and to determine the optimal chemical amount. Most common techniques are jar testing, particle size analysis (PSA), turbidity analysis, optical density, measuring conductivity and zeta potential. Method is depended on the application. Despite the particles to be flocculated, principles for optimising the process are the same. (Aldajani & al., 2021; Dayarathne & al., 2021)

### **3.2 Parameters used in process control**

#### **3.2.1 Chemical type and concentration**

Flocculant type and concentration are the most impactful process parameters for coagulation-flocculation process. Cost plays a key role in selecting the coagulation and flocculation agent. Most companies do not have resources to do extensive testing with different chemical options and combinations. Therefore, the less expensive options such as ferric and aluminium salts are most widely used. (Dayarathne & al., 2021)

With too low concentration there will still be fine particles present. This will lead to difficulties in sedimentation or filtration. It may also decrease filtrate or supernatant quality. With optimal flocculant concentration all fine particles are bridging to other particles increasing average particle size and decreasing the number of particles. As seen in Figure 1. flocculant type has a huge effect on the success of the coagulation-flocculation process. Wrong type of flocculant may not have a large impact on the number of particles as with flocculant A in below. With flocculant B the effect is major, but the flocs are not stable. With flocculant C particle count decreases drastically and formed floc are rather stable. (Mettler-Toledo, 2021; SSWM, 2021)

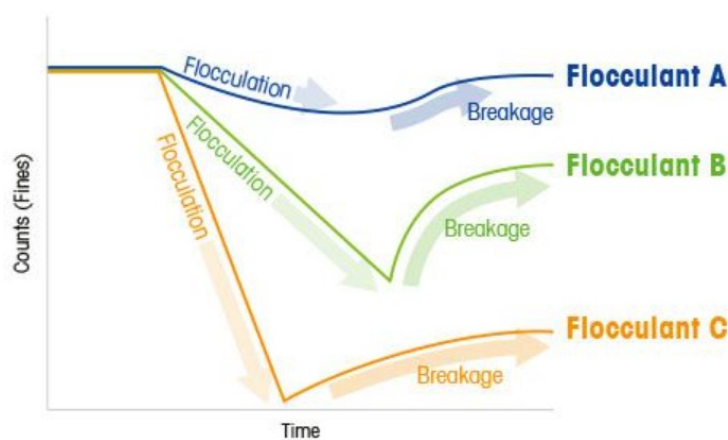


Figure 1. Effect of flocculant type. (Mettler-Toledo, 2021)

### 3.2.2 Mixing

Shear forces and mixing time have significant effect on flocculation efficiency and floc stability. Solution composition leads to different type of flocs and all flocs have their specific strength and agglomeration time. Therefore, to prevent floc breakage or incomplete floc formation, stirring speed and time should be optimised for all processes. (Aldajani & al., 2021)

In coagulation step there is no risk in over-mixing but on the contrary to coagulation macro flocs are sensitive. Over-mixing in flocculation is the point where high shear forces begin to break the floc structure and once macro floc collapses it is almost impossible to reform it. Floc breakage due to shear forces is illustrated in Figure 2. Adding three types of flocs and stirring with 250 rpm increases the median particle size significantly. Increasing stirring to 750 rpm breaks the flocs and median particle size decreases. When

slowing the stirring back to 250 rpm only part of the flocs is reformed. (Aldajani & al., 2021)

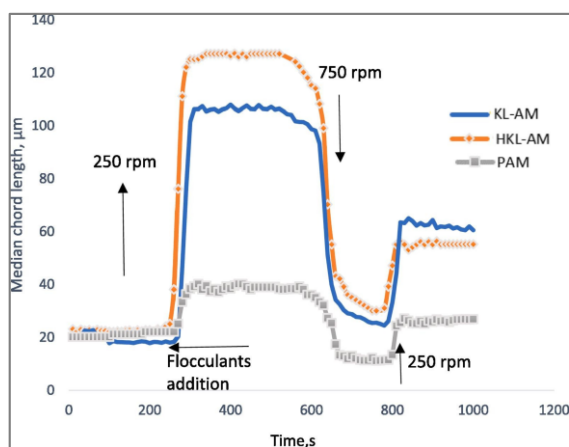


Figure 2. Effect of shear forces on three floc types. (Aldajani & al., 2021)

### 3.2.3 pH

pH can impact both the liquid which is to be flocculated but also the coagulant or flocculant agent and their interaction. Change in pH may decrease the charge of the material to be flocculated which leads to reduced efficiency in neutralisation phase and formation of micro flocs. pH is also critical in formation of bridges between metal coagulants and polymeric flocculants. Change in these chemicals' charges can lead to looser macro flocs. For metal salt coagulants most effective process pH range is pH 4.5 – 6.5. As the chemical itself can be acidic buffer needs to added prior adding these chemicals. (Dayarathne & al., 2021)

### 3.2.4 Turbidity

High turbidity materials require less chemicals compared to low turbidity materials. High turbidity means more particles and more collisions between the particles. High frequency in collisions leads to increased chance in micro floc and macro floc formation. In low turbidity materials collision are rare and therefore requires more chemical to increase the frequency in collisions. (Dayarathne & al., 2021)

### 3.2.5 Temperature

Temperature can have an impact in coagulation and flocculation efficiency. At low temperature particles have less motion which decreases frequency in collisions. Collisions also have lower energy which can lead to formation of weaker flocs. More irregular shaped floc has also been reported at low temperatures. The effect of temperature can be compensated with higher chemical dosage. (Dayarathne & al., 2021)

### 3.3 Methods for optimisation

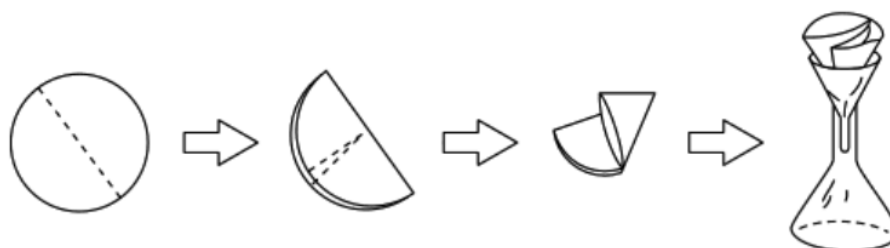
#### 3.3.1 Jar testing

Jar testing is the most conventional way to optimise coagulation-flocculation process. It is essential that the jar testing procedure mimics closely the actual process in larger scale. If the large-scale process cannot be downscaled the results from jar testing can be misleading which is the main issue also with the testing. Jar testing is widely used in wastewater treatment and there is commercial equipment available. With the commercial equipment in Picture 3, six parallel tests can be performed, and mixing can be set accurately. More simple assemblies are also possible. (Bratby, 2016)



Picture 3. Jar testing equipment for testing coagulation-flocculation process in wastewater treatment plant. (Ali & al., 2009)

All jar testing equipment consists of stirrer, jar, and filtration equipment if that is the next process step. Stirrer can be motor driven or magnetic but the stirring needs to be adjustable. Jars should be as large as possible to ease the chemical dosing. Tall jars give more reliable results in settling. Filtration equipment depends on the large-scale unit operation but in simplest it may be filter paper and funnel placed over a measuring glass or flask as seen in Picture 4. (Bratby, 2016)



Picture 4. Simple filtration system for jar testing. (Bratby, 2016, p. 366)

Regardless of the parameter under investigation, jar testing procedure remains the same. A sample is placed in the jar and mixing is set to high speed and pH is adjusted if needed. At high speed, the coagulant agent is added. This mimics the rapid mixing phase and is continued for a set period. After rapid mixing stirring is set to slow speed and flocculation agent can be added. After slow mixing stirrers are stopped and the sample is allowed to settle or filtrated immediately. Relatively large samples ranging from millilitres to hundreds of millilitres are taken from supernatants or filtrates and the best dosage or other parameters are determined after measurements such as turbidity. (Bratby, 2016)

### 3.3.2 Conductivity and ionic strength

Mortadi & al. (2020) explains utilizing conductivity as a main process controller for monitoring flocculation process. High conductivities are due to the charges of the free particles in suspensions. After flocculation, the number of free particles should decrease leading to decrease in conductivity. Excess amount of the flocculant increases the number of ions and consequently the conductivity. Shifts in conductivity might be very small and therefore accurate measurements are needed. Conductivity can be calculated into ionic strength and relaxation time. Ionic strength indicates the number of free ions. Ionic strength should decrease in the same respect as conductivity. Figure 3. shows how

ionic strength and relaxation time are depended on flocculant amount. With 10 mg/l of flocculant, the lowest level of ionic strength and the highest relaxation time is achieved. With higher concentrations ionic strength slightly increases due to the free ions from the flocculant and relaxation time decreases sharply. (Mortadi & al., 2020)

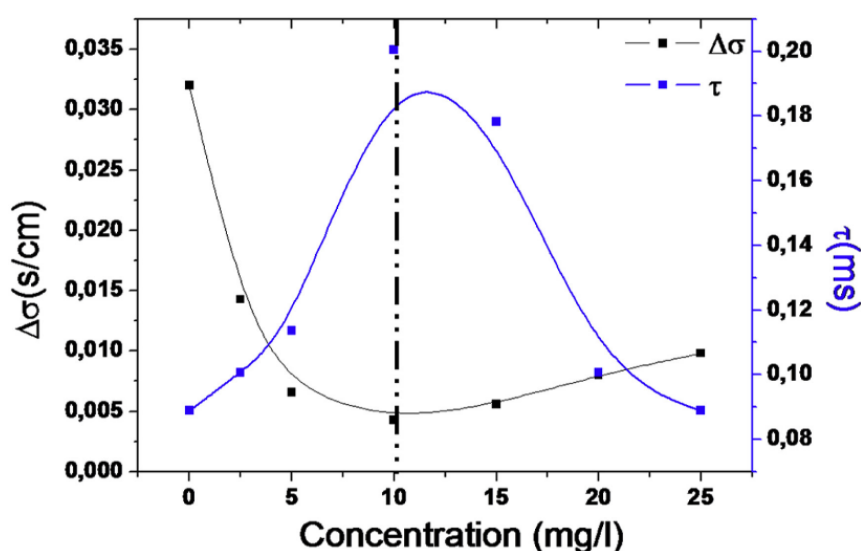


Figure 3. Change of ionic strength  $\Delta\sigma$  and the relaxation time ( $\tau$ ) as a function of the coagulant concentration. With the optimal dosage, the lowest level of ionic strength and the highest relaxation time is achieved. (Mortadi & al., 2020)

### 3.3.3 Zeta potential

A zero-point indicates a situation where there is no positive or negative charge in the measured system. In a coagulation-flocculation process it is the point where charges are completely neutralised with a coagulant agent. The Zero-point is estimated with zeta potential. The zeta potential is measured *ex-situ* with electrophoresis. It is time consuming method and therefore not widely used. For processes where neutralisation and surface charge do not have a significant role, measuring the zeta potential is not feasible in optimisation. (Dayarathne & al., 2021)

### 3.3.4 Turbidity measurement

Turbidity measurement indicates the relative clarity of a liquid and can be used in systems where settling occurs after coagulation-flocculation process. Turbidity

measurement is suitable only for small particles which are maximum of some tens of microns and is not accurate method in estimation particle amount and size. However, the method is very sensitive for changes. It is also quick and inexpensive. It is possible to calculate flocculation efficiency (FE) based turbidity measurement:

Equation 1. Flocculation efficiency calculated with turbidity measurements. NTU refers to the nephelometric turbidity unit which is measured with turbidity meter. Turbidity of a control measurement in the equation is turbidity of the supernatant without flocculation after settling. (Ajao & al., 2021)

$$FE(\%) = \frac{NTU_{test} - NTU_{control}}{NTU_{control}} * 100\%$$

$NTU_{test}$  = turbidity of supernatant after flocculation and settling time

$NTU_{control}$  = turbidity of supernatant after settling time

In principle after coagulation-flocculation process turbidity should decrease in the supernatant. Overdosing may also increase turbidity due to flowthrough of the chemical and it is important to recognise whether increase in turbidity is due to under or overdosing. There are *in-situ* probes available for measuring turbidity during the process. (Ajao & al., 2021; Aldajani & al., 2021; Chianese, A. & al., 2012)

### 3.3.5 Optical density

Flocculation efficiency can be also calculated according to Equation 2 using optical density measurements in systems where the aim is to flocculate cell material and turbidity measurements are not accurate enough. The optical density is measured with spectrophotometer in quartz cuvettes at 680 nm ( $OD_{680}$ ). (Hadiyanto & al., 2021)

Equation 2. Flocculation efficiency calculated with optical density measurements.  $OD_t$  is the density of supernatant after flocculation and settling and  $OD_{t0}$  density of supernatant after settling but without flocculation. (Hadiyanto & al., 2021)

$$FE(\%) = 1 - \frac{OD_t}{OD_{t0}} * 100\%$$

$OD_t$  = optical density of supernatant after flocculation and settling time

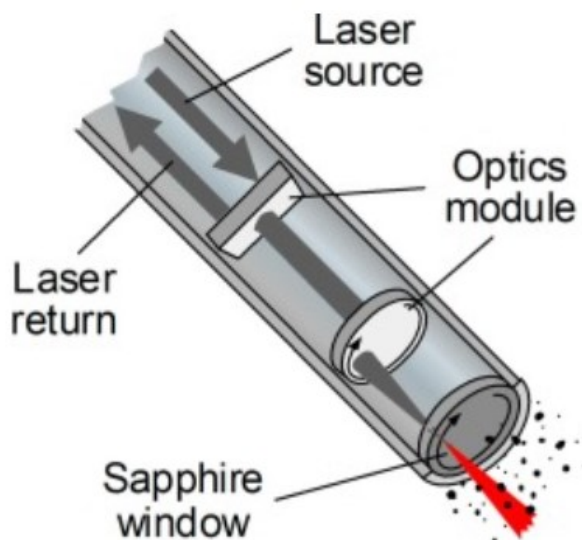
$OD_{t0}$  = optical density of supernatant after settling time

The optical density is measured at 2/3 of the height of the cell broth after the flocculation and settling period. The initial concentration of cells can also be evaluated with  $OD_{680}$  measurement to estimate the flocculant agent amount. Optical density measurement is suitable for cell materials which do not contain insoluble media components which interfere the measurement. It is widely used in process control of microalgae flocculation. (Hadiyanto & al., 2021)

### 3.3.6 Focused beam reflectance measurement

Focused beam reflectance measurement (FBRM) is the most suitable for coagulation-flocculation process from all particle size analysis methods. FBRM is an in-situ probe-based method for the determination of the chord length of particles. Chord length is an estimation of particle dimension and is defined as straight-line distance from one edge of a particle to another. FBRM probe produces a solid-state laser light that is focused to a small area at a constant distance from the probe window as seen in Picture 5. Motor is used to rotate optics module such that the rotating beam of laser is constantly scanning passing particles. The particles backscatter the laser light back to the probe and on to light detector. Detector uses this information in calculation of the chord lengths and chord length distribution (CLD). Particle size distribution cannot be calculated straight from the CLD since the shape and orientation of the particles is random in the liquid. This technique has been used for monitoring and controlling crystallization process,

solidification of micro-particles, granulation, and granulation-drying-milling process. (Chianese, A. & al., 2012; Dayarathne & al., 2021; Sankaranarayanan & al., 2019)



Picture 5. Schematic of a FBRM probe: solid-state laser light is focused to small area at a constant distance from the sapphire window. Particles that pass the window backscatter the laser light back to the probe and on to light detector through optical modules. (Kyodaab & al., 2019)

FBRM technique can effectively be used for the determination of the particle size changes and kinetics. The probes measure these lengths each second or as often as is defined and CLD acts as a fingerprint for every timepoint. It is statistically robust because the probe counts several thousand of particle per second. FBRM can be used in wide range of temperature and pressure. Particle concentration does not either limit the use of FBRM. FBRM is sensitive for fine particles which might be unnoticed with other techniques. Limitation for the use of FBRM is stirring conditions. Stirring can affect the measurement and should therefore be constant throughout the process. Transparent particles which do not backscatter are uncounted with FBRM. FBRM can also not differentiate particle shapes (Chianese, A. & al., 2012, Sankaranarayanan & al., 2019)

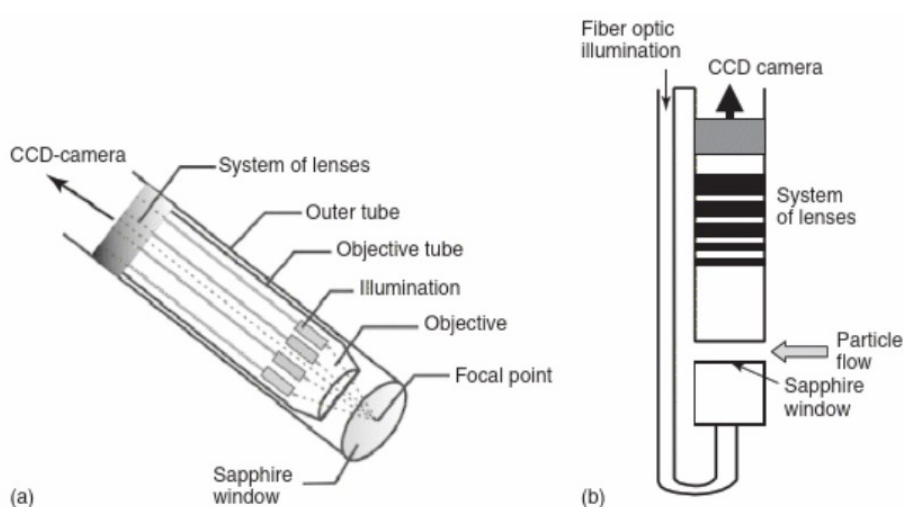
Changes in the particle distribution indicates changes in the system. Before coagulation-flocculation process there should be more fine particles and their amount decreases during flocculation. Average particle size also increases. FBRM can also be used to monitor flocculation breakage. (Dayarathne & al., 2021)

### 3.3.7 Particle vision and measurement

Another particle size analysis method is particle vision and measurement (PVM) also known as analysis by imaging. It relies on rapid image analysis and is known to have potential in flocculation process control and optimisation, but more studies are needed. PVM can analyse particle shape, size, and count. Compared to FBRM it is more suitable for low concentration systems. PVM can be measured only *in-situ* and is therefore quick method for process control and reduce the risks of overdosing since observations are made instantly. (Dayarathne & al., 2021)

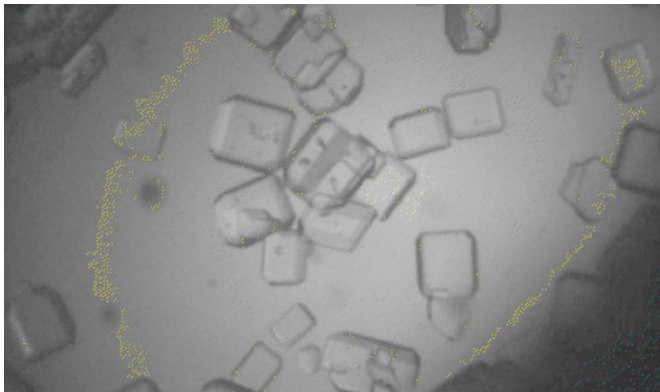
Measuring systems scan and image the liquid as it passes through the measuring window. Most commercially available systems consist of light source, detection system (probe) and image analysis system. Light source is often solved with fibre optics which run through a probe. Round shaped light source illuminates the particles with flashing light. Short illumination time helps avoiding blurry images caused by movement of the particles and prevents samples from heating up. The illuminating system determines the quality of the images. (Chianese, A. & al., 2012)

Front-end illuminator illustrated in Picture 6 illuminates the particles on the same side as they are detected. This simplifies probe design and is therefore very common. Drawback of front-end design is that particles closer to the window often block particles behind, images are not as high quality and poorly defined outlines of the particles. (Chianese, A. & al., 2012)



Picture 6. a) Schematic of front-end illuminating PVM probe. b) Layout of the probe. (Chianese, A. & al., 2012, p. 41)

Option for the front-end design is separating the light source and the detector. In these systems higher quality images are obtained as seen in Picture 7. By separating the functions parallel measurements of illuminating and detecting are possible. Particle positions do not affect the result since they are seen in the background. Hydrodynamic conditions affect this system design and system design is more complicated and their physical size increase. This system layout is feasible only for low concentration liquids and thus it not applicable in coagulation-flocculation processes. (Chianese, A. & al., 2012



Picture 7. High quality image of Ammonium Sulphate taken by PVM where light source and detector are separated. (Chianese, A. & al., 2012, p. 42)

The detection system usually consists of high-resolution CCD camera. High resolution means high magnification in PVM systems. As magnification increases the depth of the measurement field decreases which may be problematic with large particles that can overlap the whole field and smaller particles. Post-processing of the images corrects the issues to some extent. High resolution pictures need very short illuminating times which are difficult to do in practice. (Chianese, A. & al., 2012)

Image analysis is performed with software and algorithms. Used algorithm depends on the system provider. In all data is retracted from the images by image segmentation. This means that the particles are separated from the background. In image segmentation every pixel is analysed and pixels with same label are part of a same particle. Algorithms are used to improve the image quality, perform background correction, improve sharpness, detect particle boundaries and overlapping, and removing noise. (Chianese, A. & al., 2012)

## 4 CELL SEPARATION OF FERMENTATION BROTH

### 4.1 Solid-liquid separation by sedimentation and centrifugation

#### 4.1.1 Principle

Sedimentation and centrifugation are an early-stage downstream unit operations in bioprocessing. Aim of cell separation is to capture the target biomolecule and remove the host cells and partially impurities such as cells debris and process related impurities such as insoluble culture media components. They are mainly used after the addition of a flocculant to broth or cell lysates since it is useful to increase the particle size by flocculation to make the sedimentation or filtration step more efficient. (Esmailnejad-Ahranjani & al., 2022; Harrison & al., 2015)

The productivity, purity, recovery of the desired product, and yield are the key parameters to consider when developing sedimentation or centrifugation. They are commonly optimized by running the centrifuge at very high rotational speeds and high volumetric flow rates. There is a risk that if the feed flow rate is too high the cells will escape from the centrifuge or the high shear forces will cause severe cell damage or even cell lysis. If cell lysis occur impurities inside the cell can leak and add load to following purification steps. (Esmailnejad-Ahranjani & al., 2022)

Sedimentation is the movement of particles in an inertial field. Various theories of sedimentation of flocs have been proposed since this is vastly exploited in the water-processing industry. The inertial field is in sedimentation gravitational acceleration ( $g=9,8 \text{ m/s}^2$ ). In centrifugation the inertial field is the centrifugal acceleration presented in Equation 3. The acceleration can vary between  $1 \times g$  to  $100\,000 \times g$ . (Harrison & al., 2015)

Equation 3. Centrifugal acceleration. (Harrison & al., 2015, p. 180)

$$\text{centrifugal acceleration} = \omega^2 R$$

$\omega$  = angular velocity

R = distance of the particle from the centre of the rotation

Applications of sedimentation and centrifugation are widespread. Sedimentation by gravity is most commonly used in wastewater treatment after coagulation-flocculation step. Centrifugation is used in biotechnology industry such as vaccine production and in clinical laboratories. In bioprocessing, the most frequent applications are clarification of broths and lysates and the collection of cells. In bioprocessing sedimentation includes settling tanks and tubular centrifuges for batch processing, and continuous centrifuges such as disk centrifuges. Laboratory scale centrifuges for small samples can be found in most research laboratories and are frequently used for processing of small cell cultures. (Esmailnejad-Ahranjani & al., 2022; Harrison & al., 2015)

#### 4.1.2 Sedimentation and centrifugation techniques

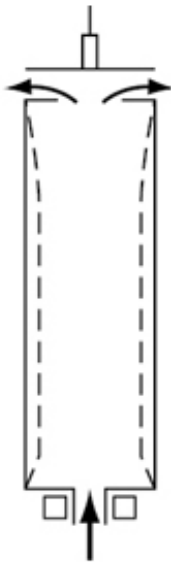
Particles and cells can be separated at large scale in continuous or in batch centrifuges. Continuous-flow centrifuges have been widely employed due to their operational robustness, and ability to process large volumes with high solid content or biomass. The most exploited methods at production scale are tubular bowl centrifuge and the disk-stack centrifuge. Ultracentrifuges also exist but they are mainly used in analytical and preparative work. The tubular and the disk type centrifuges are the most commonly found in the bioprocess industry since they are usually involving the recovery of a proteins produced by cells. (Esmailnejad-Ahranjani & al., 2022; Harrison & al., 2015)

Other types of centrifuges such as decanter and basket centrifuges are typically used for particles that sediment relatively rapidly such as crystals and are not suitable for cell separation. (Harrison & al., 2015)

Tubular centrifuge is a batch type centrifuge where solids sediment on the wall of the bowl, and feed continues until the chamber is full. After this point the bowl is emptied.

The material is fed from one end and the filtrate is recovered from the opposite end. This type of centrifuge works well for particles which have relatively low sedimentation coefficient and that must be recovered, such as protein precipitates and microbial cells. (Harrison & al., 2015)

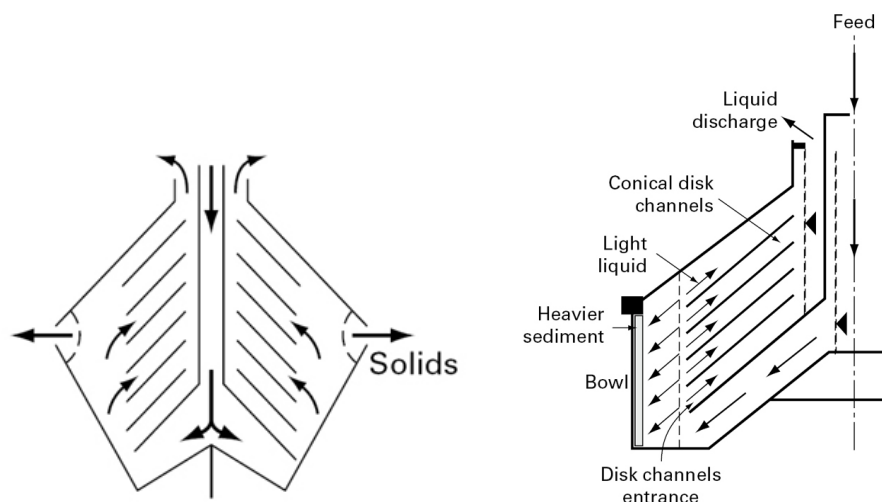
Since solids build up on the wall of the bowl, the inner radius of the bowl decreases leading to decrease in the maximum g-force and residence time. Therefore, in order to continue capturing the particles, the flow rate of the feed needs to be decreased as g-forces decrease. The centrifuge is usually fed until particles flow through to the other end. At this point solids take already 80 % of the bowl volume and there not enough g-forces to continue the process. To continue operation, the solids need to be discharged. (Harrison & al., 2015)



Picture 8. Schematic of tubular centrifuge. (Harrison & al., 2015, p. 187)

Disk centrifuge is continuous or batch type of centrifuge that have a relatively high sedimentation area per volume. In batch type nozzles are closed and the sediment is collected to the outer wall of the bowl. In continuous type the nozzles which are located in the outer parts of the bowl are open and the heavy sediment flow out of the centrifuge. Disk centrifuges are used for the centrifugation of cells and cell lysates. Advantage of the system is that it is a closed system which prevents escape of aerosols. (Harrison & al., 2015)

A disk centrifuge is a system which consists of rapidly rotating concentric inverted cones which are placed close together. This minimizes the time to capture dense particles or liquids at relatively high dimensionless accelerations. In disk centrifuges the liquid is fed next to the centre and forced towards the bottom of bowl. Pressure forces the suspension upward and the heavier fluid is forced through holes at the end of each disk channel until it reaches walls of the bowl. The lighter fluid flows up the disk channels and out of the centrifuge. (Harrison & al., 2015)



Picture 9. Schematic of disc centrifuge and the liquid flow. (Harrison & al., 2015, p. 187-190)

## 4.2 Solid-liquid filtration

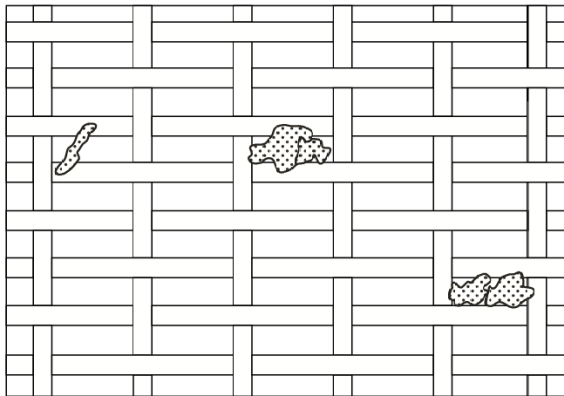
### 4.2.1 Principle

Cell separation of fermentation broth is part of solid-liquid filtrations. Based on Perlmutter (2015) there are two main principles in solid-liquid filtrations:

Either the solids have a tendency to go one way and the liquid the other way (i.e., separation) or one must find a hole smaller than the solids which one wishes to capture (i.e., filtration).

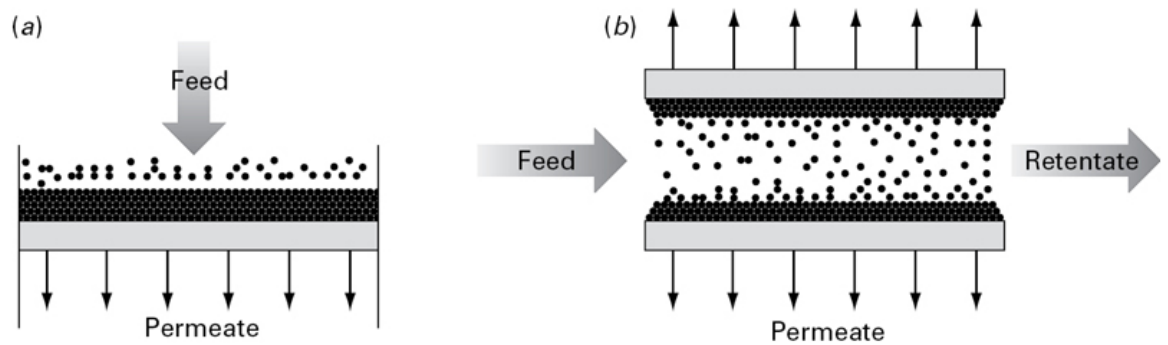
All solid-liquid filtration techniques fall into these two categories. Same material can be separated or filtrated with several different techniques and the choice can be depended on several parameter such as filtration flux, product quality and already existent equipment. (Perlmutter, 2015)

Solids can be removed from liquids either with cake filtration or with the depth of filter medium. Filter media itself, filter cake and filter aids are all part of the depth of the filter media. There are three mechanisms to remove solids by filtration: inertial impaction, diffusional interception, or direct interception. Inertial impaction refers to particles taking the path with the least resistance meaning a straight line through the filter media and cake. Larger particles tend to deviate more from the straight line due to collisions with the filter media. Small particles tend to be removed through diffusional interception. In this mechanism the solid particles are interacting with the liquid molecules. These collisions make the solids to deviate from their path. Direct interception is the most common mechanism in removing solids. In the depth of the filter medium defines the pores openings. Particles larger than the pore are removed when they encounter small opening as seen in Picture 10. Particles smaller than the opening are removed with bridging. In bridging several particles strike the pore simultaneously and are removed. (Flickinger M., 2013; Perlmutter, 2015)



Picture 10. Direct interception. Small particles are removed if they hit opening simultaneously. (Perlmutter, 2015, p. 7)

Filtrations can be divided according to the direction of the fluid feed in relation to the filter medium. In dead-end filtration which is also known as conventional filtration the fluid flows perpendicular to the medium. In crossflow filtration or tangential flow filtration the fluid flows parallel to the medium. Conventional and crossflow filtration are illustrated schematically in Picture 11.

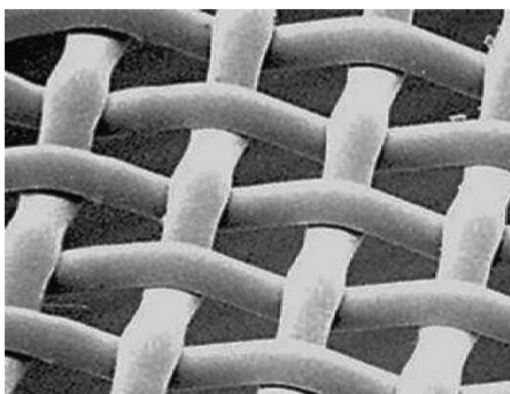


Picture 11. Dead-end filtration (a) compared to crossflow filtration (b). (Harrison & al., 2015, p. 143)

#### 4.2.2 Filter media

Filter medias can be divided into two groups based on the material: synthetic cloth and metal. Which one to choose depends on the process requirements such as chemical and thermal requirements and characteristics of the solid-liquid material. (Perlmutter, 2015)

Synthetic cloths are made from polyester, nylon polypropylene and other synthetic polymers. Synthetic filter medias can be divided into two groups based on the degree of openness: plain waves (Picture 12) and closed waves. Plain waves have nearly visible openings larger than 200 micrometers and closed waves' have openings of 1-200 micrometers. (Perlmutter, 2015)



Picture 12. Close-up to synthetic plain wave with large openings. (Perlmutter, 2015, p. 11)

Synthetic cloths can be monofilament or multifilament. Monofilaments are regular shape and solids are less likely to adhere on the surface due to the smoothness of the surface.

For the same reason they are easier to clean. In multifilament cloths fine strands are twisted together into threads. The surface of the thread is coarse and have elasticity. Multifilaments are harder to clean, and they trap solids more easily. There are also filter media that are mix of both. (Perlmutter, 2015)

Metal medias are made of stainless steel and different alloys such as nickel and titanium. Metal cloths can be single layer or multilayer. Single layer metal medias are similar to synthetic cloths in structure. Multilayer metal cloths are more complicated, and the openings are small. In multilayer structure the porosity is uniform and more controlled. Multilayers are typically two, three or five layered. The top layer typically acts as protective layer, middle layer determines the removal efficiency and bottom layer is for draining. (Perlmutter, 2015)

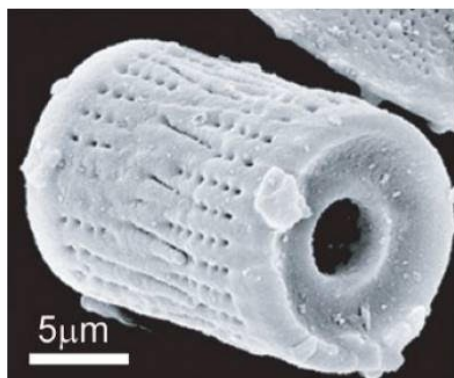
#### 4.2.3 Filter aids

Filter aids can be used as a precoat or as a body feed. Precoat is done prior the actual filtration with water or another liquid such as buffer. As a precoat, the filter aid protects the filter media against the penetration of unwanted solids, prevents clogging of the filter media and can increase the quality of the filtrate. If the solids form a layer that cannot be penetrated, the thickness of the precoat does not matter. If the solids are more fibrous and amorphous and can get into the depth of the precoat, a thicker precoat is needed. (Perlmutter, 2015)

Body feed is added straight to the liquid to be filtrated. It means that the solid layer on filter media thickens as the filtration proceeds. There is no practical way to separate added body feed from the liquid phase. In situations where filtration or another separation technique is not anymore possible for instance due to a bad filter media clogging the whole batch needs to be disposed. The combination of the two approaches is the most common. (Perlmutter, 2015)

The filter aid type should be chosen based on particle size, solids density and characteristics. The solids to be removed can also interact with the filter aid and therefore needs to be considered beforehand. Diatomite is a common filter aid. It is obtained from diatomaceous earth, and it contains silica as siliceous diatoms. These diatoms are durable in retaining their structure through long periods of time and thermal processing. Diatomite products are highly porous and have complex structure as seen in Picture 13.

They also include relatively high amounts of impurities such as alumina iron oxide, and alkaline earth oxides. (Perlmutter, 2015)



Picture 13. Structure of diatomite particle. (Sarasti, 2017, p. 12)

Another common inorganic filter aid is perlite. It is a naturally occurring volcanic glass that consists of sodium potassium aluminum silicate and can expand when heated. It is manufactured through milling after which it has a porous, complicated structure. Because its structure is not as complex as diatomite's, perlite works well in separation of coarse and large particles from liquids having high solid content. Perlite also has lower density than diatomite, which enables using less filter media. Both perlite and diatomite are widely used with depth filter sheets and pads. (Perlmutter, 2015)

There are also organic filter aids. Most common is cellulose filter air which is produced by the sulfite or sulfate processing of hard wood. Cellulose filter aids are large in particle size, which enables it to precoat a filter media easily. It is most often used in combination with diatomite. Cellulose has less complex structure compared to diatomite. More rare organic filter aids are potato starch particles, cotton linter, and polymeric fibers. These all are commonly used with diatomite because they can help in dispersing diatomite to the surface of the filter media. In some rare applications organic filter aids can be used as such. (Perlmutter, 2015)

#### 4.2.4 Principles of dead-end filtration in cell separation

Dead-end filtration is commonly used when a product has been secreted from cells to the surrounding liquid, and thus the cells need to be removed to obtain cell free liquid to which the product is dissolved. Antibiotics and steroids are often processed by using

conventional filtration to remove the cells. Conventional filtration is also often used as sterile filtration in bioproduction to remove contaminants in the product. (Harrison & al., 2015)

There are several types of dead-end filters as described in Table 2. The filters can be divided to continuous and batch type. (Harrison & al., 2015)

Table 2. Examples of dead-end filtration systems. (Perlmutter, 2015)

<b>Filter type</b>	<b>Process type</b>
Belt press filter	Continuous
Screw press filter	Continuous
Pan filter	Continuous
Vacuum belt filter	Continuous
Pressurised drum filter	Continuous
Rotary drum vacuum filter	Continuous
Disc filter	Continuous
Rotary press filter	Continuous
Tower press filter	Batch
Pressure plate filter	Batch
Candle filter	Batch
Bag filter	Batch
Cartridge filter	Batch
Tubular filter	Batch
Membrane Press filter	Batch
Plate and frame filter press	Batch

The slurry containing the cells and other particles flows towards the filter medium by applying a pressure across that medium. Simultaneously, the solids begin to build up on the filter medium as shown in Figure 4 and the liquid containing the dissolved product flows through it. (Harrison & al., 2015)

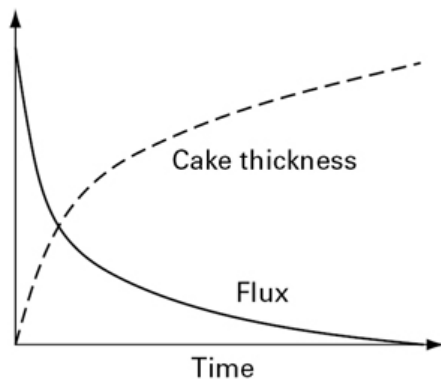


Figure 4. In dead-end filtration solids build up thickening the cake which leads to decrease in permeate flux. (Harrison & al., 2015, p. 143)

The accumulation of cells and other solids on the filter medium forms the cake. If the cell density in the slurry is high, the cake can quickly affect the filtration performance. With Darcy's law which is described in Equation 4, the flow of liquid through the cake and filtration media can be calculated:

Equation 4. Darcy's law describes flow of the liquid through the cake. (Harrison & al., 2015, p. 144)

$$\frac{1}{A} \frac{dV}{dt} = \frac{\Delta p}{\mu R}$$

V = volume of the filtrate

t = time

A = filtration area

$\Delta p$  = pressure drop through the cake and filter medium

$\mu$  = viscosity of the filtrate

R = resistance of the cake and filter medium

It is often necessary to wash the filter cake with water or a salt solution to recover as much of the product as possible with dead-end filtration. The wash should be done with more than the volume of liquid in the cake to obtain sufficient recovery. Transfer of the

product into the wash liquid occurs by diffusion, which has a slower rate than the flow of the washing liquid through the cake. (Harrison & al., 2015)

#### 4.2.5 Principles of crossflow filtration in cell separation

In cross flow filtration, the liquid flows parallel to the membrane surface, resulting in constant permeate flux at steady state as seen in Figure 5. Cross flow filtration is widely used in the variety of applications such as cell separation, removal of cell debris and viruses, concentration of cells or protein solutions, ion exchange and removal of salts. (Harrison & al., 2015)

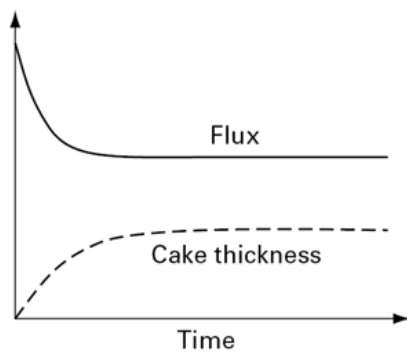


Figure 5. A Constant permeate flux in steady state cross-flow filtration. (Harrison & al., 2015, p. 143)

At steady state, the rate of convective mass transfer of solute toward the membrane surface must be equal to the rate of mass transfer of solute by diffusion away from the membrane surface, as described in Equation 5:

Equation 5. The rate of convective mass transfer of solute toward the membrane surface at steady state of crossflow filtration. (Harrison & al., 2015, p. 148)

$$J c = D \frac{dc}{dx}$$

J = transmembrane flux

c = concentrate of the solute

D = diffusion coefficient of the solute

Cross flow filtration can be divided into two categories depending on whether the component being filtered is soluble (proteins) or insoluble (cells and cell material). When dissolved substances such as proteins are being filtered, ultrafiltration membranes are most often used. The ultrafiltration membrane is selected so that the protein will not flow through the membrane. The retained species is carried to the surface of the membrane by the convective flow of fluid, and the concentration of the soluble protein or other substance increases. Concentration of the soluble material can be so high that it precipitates on the membrane surface and decreases the flow through the membrane. This can happen also without precipitation by increasing the osmolarity near the membrane surface that creates a gradient which resists the applied transmembrane pressure. (Flickinger M., 2013; Harrison & al., 2015)

When suspended particles or cells are present in the slurry, the particles flow to the membrane surface and may form a cake on the surface. In this situation, micro filtration membranes are used over ultrafiltration membranes. Micro filtration membranes let dissolved components pass through but particles above a certain size will remain in the slurry. (Flickinger M., 2013; Harrison & al., 2015)

## 5 MATERIALS AND METHODS

### 5.1 Background

Coagulation and flocculation chemicals and their specific dosages are not presented in this thesis for confidentiality reasons. The chemicals are referred to as a flocculant. Dosages are case-specific and are referred to plain numbers except that dosing 0 always refers to reference experiment where coagulation or flocculation chemicals are not present.

Filtration data is also presented as relative figures and can only be compared within the specific experiment set.

### 5.2 Fungal and *Bacillus* fermentation processes

Proteins such as enzymes are often produced with submerged fermentations. In submerged fermentations, microorganisms are grown in liquid medium containing C-source, N-source, and other nutrients such as trace elements. Oxygenation is done by using agitation and aeration. Nutritional requirements of the microorganisms are complex, and it varies between microorganisms and thus fungal fermentations require different substrate and other components compared with *Bacillus* fermentations. Also, different strains can have very specific requirements. (Todaro, C. & al., 2014)

Two *Trichoderma reesei* and two *Bacillus subtilis* processes were selected for this study. *T. reesei* strains were fermented in laboratory and pilot scale, *Bacillus* fermentations in pilot scale. The different scale might cause some upscaling effect and differences in the results. The processes are presented in below Table 3 with coding for individual test series.

Table 3. Selected processes and coding.

Process code	Production strain	No. of laboratory scale cultivations	No. of pilot scale cultivations	Coding for test series
A	<i>Trichoderma reesei</i>	1	1	A1, A2
B	<i>Trichoderma reesei</i>	1	1	B1, B2
C	<i>Bacillus subtilis</i>	0	2	C1, C2

The fungal fermentations are expected to have different particle size distribution compared with *Bacillus* fermentations due to the different medium components and cell structure. Fungal microorganism often grows in filamentous form and *Bacilli* are single cell rods. (Todaro, C. & al., 2014)

### 5.3 Equipment

#### 5.3.1 Particle size analyser

Particle size measurements were conducted with Mettler-Toledo's Easy Viewer 100 in-situ particle size analyser. It consists of Easy Viewer 100 probe visualised in Picture 14 and iC Vision software. The device is meant for laboratory use only. Easy Viewer 100 is a particle vision and measurement-based system which has front-end illuminator with sapphire window. The field of view is 1000  $\mu\text{m}$  x 1000  $\mu\text{m}$  and it can detect particles over 1.5  $\mu\text{m}$  in chord length. The probe also measures turbidity. (Mettler-Toledo, 2021)

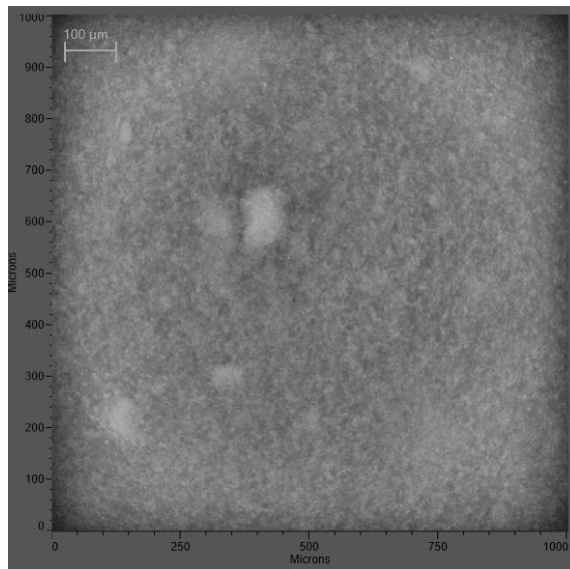


Picture 14. Easy Viewer 100 probe. Sapphire window is located in the tip of the probe. (Mettler-Toledo, 2021)

iC Vision software analyses the captures with Boundary algorithm which is based on edge detection. The algorithm binaries the images and particles are the set of pixels that have at least one neighbour outside that region. Changes in pixel intensity differentiates particles from another. Particle size is then calculated based on the pixels by shifting the

inter-pixel boundary by one-half pixel towards right and downwards. (Chianese, A. & al., 2012; Liow, 1991)

The software reports a chord length histogram and visualises them with the microscopic images seen in Picture 15. End-user can define how often a measurement is saved and displayed and whether all particles are counted or just the particles that are in-focus.



Picture 15. Microscopic picture of fermentation broth in iCVision software taken by the Easy Viewer 100 probe.

### 5.3.2 Lab scale pressure filter for cell separation

The equipment used in the experiments was Labox25 pressure filter by Larox Outotec. The filter system is designed to evaluate filtration properties at laboratory scale prior actual production scale.

Labox25 mimics at micro scale production size tower press filter. Tower press filter and Labox25 both are batch type dead-end filters. In tower press filters there is vertically stacked chambers. A cloth zigzags through the stack forming chambers. Filtration itself is operated by hydraulic pressure up to several bars. At the end of every filtration cycle the cake is discharged by moving the cloth back to start position. Tower press filters are mainly used for dewatering, but it can be also used the opposite way where the liquid is the product, and the cake is the by-product. (Perlmutter, 2015)

Labox25 is a simplified version of a full-scale tower press filter. With Labox25 4 bar working pressure is applied to a piston which slowly slides inside a cylinder. Whilst moving, the piston pushes the filtered material through a filter medium into a collection tube. Solid cake is formed between the piston and the cloth and is manually discharged. Labox25 has a working volume of 130 ml.

#### 5.4 Experimental set-up

The workflow of the experimental part is presented in Figure 6. Every test and measurement were performed separately to obtain similar conditions for all. The fermentation broth was weighted to a beaker which was placed on a magnetic stirrer with high stirring speed. Easy Viewer 100 probe was placed in the broth and measurement was begun with iC Vision software prior to the flocculant addition.

Settings of iC Vision software used in the measurements are presented in Table 4. Autofocus ON indicates that only particles in focus are counted and measured. Pictures and measurements were saved every 2 seconds since the changes are rather quick in flocculation and 2 seconds was the shortest available interval. By adjusting front lighting to 40 % better quality pictures were obtained. These parameters were tested and decided in the beginning of this study and were used in every measurement to obtain comparable data.

Table 4. Main settings of the Easy Viewer 100 probe and iC Vision software for all experiments.

<b>Setting</b>	<b>Values</b>
Autofocus	ON
Front lighting power	40 %
Save interval	2 seconds
Counts	In-focus particles
Measuring system	Chord length
Particle size classes	< 50 $\mu\text{m}$ , 50 – 300 $\mu\text{m}$ , > 300 $\mu\text{m}$

After the chemical addition stirrer speed was decreased to lower level to enhance macrofloc formation and to prevent floc breakage. After several minutes the measurement and stirring was stopped. The cell separations were performed after short standing time which was equal for every experiment. Filtrate amount was measured

every 1 minute to obtain filtration curves comparing different flocculant dosages. After filtering the whole batch, turbidity was measured from the filtrate to estimate filtrate quality and filtration fluxes were calculated. The fluxes are presented in relative form.

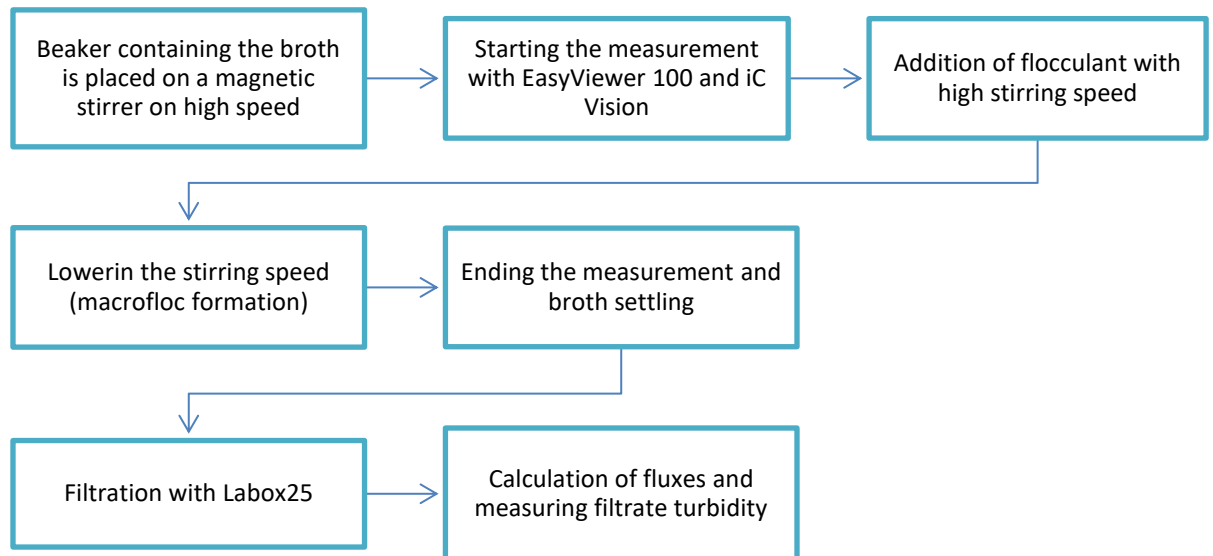


Figure 6. Workflow in the experimental part. Every measurement and filtration were performed separately.

Comparison is made in every experiment to dosage 0 which indicates a process where flocculation has not been performed prior cell separation. Numbers ranging from 1 to 4 indicates a test series where four different dosages have been tested. When 0 always indicates to 0 % of added flocculant numbers from 1 to 4 do not refer to any specific concentration. The number from 1 to 4 refers only to an individual test in that test series.

The test series are referred as letter and number combinations which are presented in table 3. For instance, test series A1 and A2 are from different fermentations but with the same fungal strain.

## 6 RESULTS

### 6.1 Fungal processes

#### 6.1.1 Optimising flocculation and cell separation of A1

Tests were carried out from one laboratory scale (A1) and one pilot scale (A2) fermentation. Coagulation and flocculation were performed with one flocculant agent in four different dosages. Dosages were determined for A2 according to results from A1. All tests were filtrated with Labox25.

The best filtration performance was achieved with dosage 2 in A1 as seen in table 5. The turbidity of the filtrate increases whilst the flocculant amount increases which can indicate flowthrough of the flocculant agent. The numbers in the column Flocculant Dosage are equivalent to the legend of Figure 7 and Figure 8.

Table 5. Filtration data for test series A1.

Flocculant dosage	Relative filtration flux [%]	Filtrate turbidity [NTU]
0	100	540
1	163	560
2	181	640
3	142	700
4	132	720

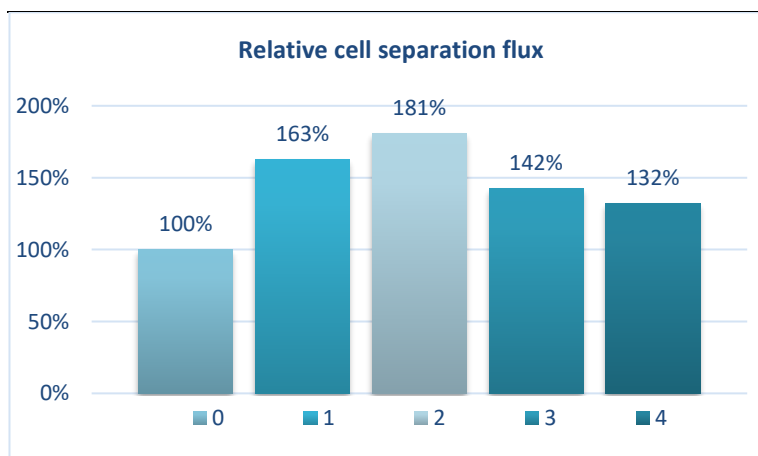


Figure 7. Relative fluxes for test A1.

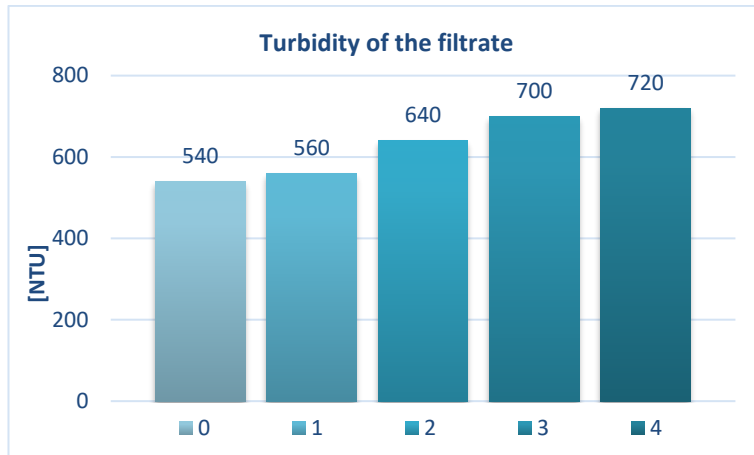


Figure 8. Turbidity of A1 filtrates.

With the most efficient flocculant dosage particle count increased during the rapid mixing phase and continued during slow mixing phase as seen in Figure 9. With lower dosage the count increased during rapid mixing and decreased during slow mixing. With higher dosing particle counts were comparable before flocculation and after slow mixing. According to the curves there is only relatively minor differences before and after flocculation in the chord length distributions, only the counts differed slightly. Rest of the figures can be seen in appendix 1.

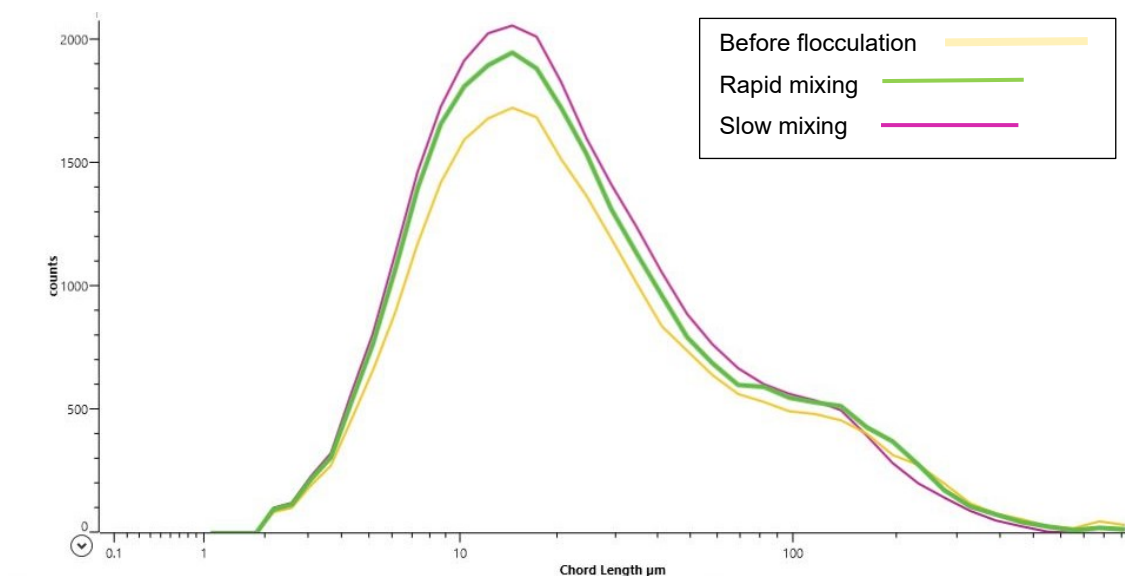
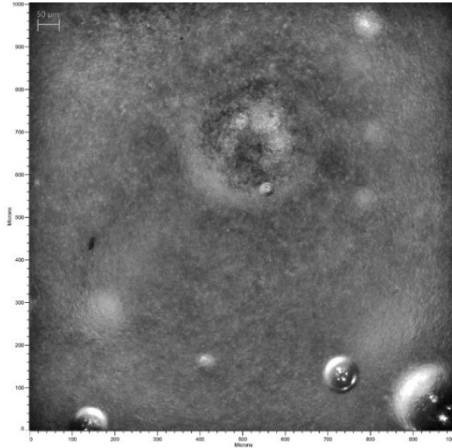
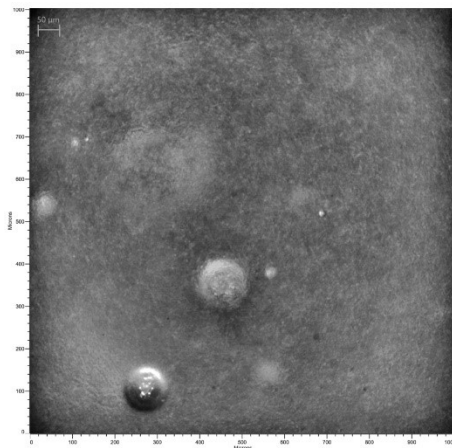


Figure 9. A1 with flocculant dosage 2. Number of count increases but no difference can be seen in chord length.

Pictures taken by the Easy Viewer 100 probe shows bubbles in the broth, but the flocculation cannot be seen clearly from the Pictures 16 (before flocculation) and 17 (after flocculation).



Picture 16. Capture from iC Vision before flocculation of A1.



Picture 17. Capture from iC Vision after flocculant dosage 2 and slow mixing (A1). No clear visual flocculation.

### 6.1.2 Optimising flocculation and cell separation of A2

Narrower flocculant amount range was chosen for A2 based on the results with A1. With A2 the best filtration performance was achieved with dosage 3. The amount of flocculant is the same as in dosage 2 with A1. The turbidity of the filtrate increases whilst the flocculant amount increases which can again indicate flowthrough of the flocculant agent.

The numbers in the column Flocculant Dosage are equivalent to the legend of Figure 10 and Figure 11.

Table 6. Filtration data for test series A2.

Flocculation dosage	Relative filtration flux [%]	Filtrate turbidity [NTU]
0	100	480
1	131	470
2	139	580
3	148	590
4	124	595

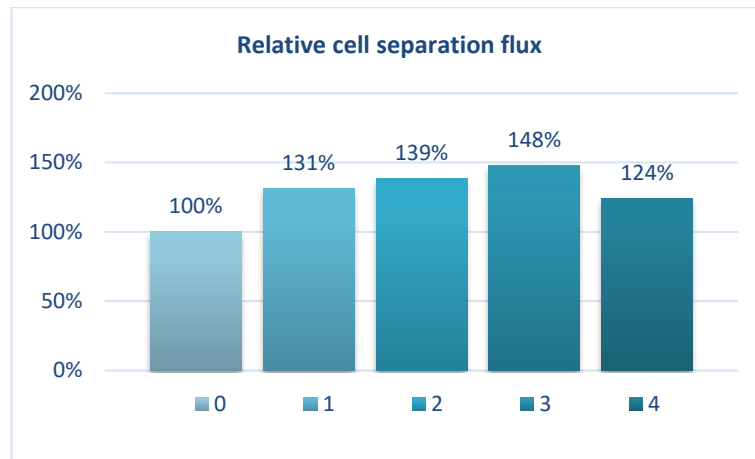


Figure 10. Relative cell separation fluxes for A2.

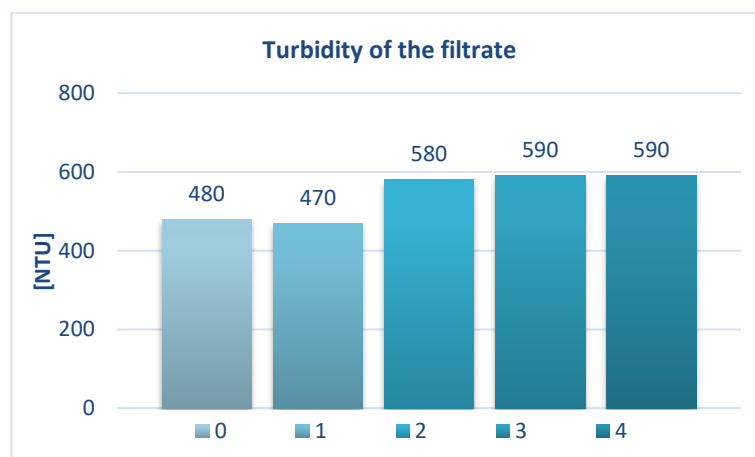


Figure 11. Turbidity of A2 filtrates.

With the most efficient flocculant dosage particle count increased during the rapid mixing phase and continued during slow mixing phase as seen in Figure 10. With dosage 1 the count increased during rapid mixing and decreased during slow mixing. With dosage 2 and higher the counts were also stable, but filtration flux decreased, and turbidity of the filtrate increased. According to the curves there is only minor differences in the chord length distributions, only the counts differed slightly before and after flocculation. Rest of the figures and pictures can be seen in appendix 1.

Pictures were taken by the Easy Viewer 100 probe. They are very similar to A1 photos and no difference or signs of flocculation can be seen from them.

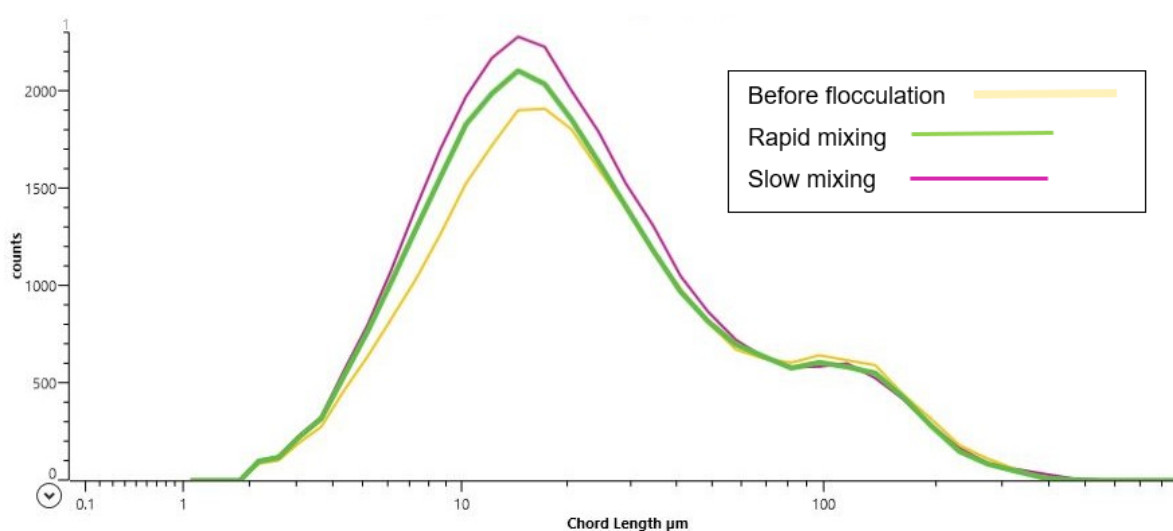


Figure 12. A2 with flocculant dosage 3. Number of counts increased but no difference can be seen in chord lengths.

### 6.1.3 Optimising flocculation and cell separation of B1

Tests were carried out from one laboratory scale (B1) and one pilot scale (B2) fermentation. Coagulation and flocculation were performed with one flocculant agent in four different dosages. Dosages were determined for B2 according to results from B1

The best filtration performance was achieved with dosages 3 and 4 with the B1. The turbidity of the filtrate increases significantly only with the highest dosage 4. The numbers in the column Flocculant Dosage are equivalent to the legend of Figure 13 and Figure 14.

Table 7. Filtration data for test series B1.

Flocculant dosage	Relative filtration flux [%]	Filtrate turbidity [NTU]
0	100	41
1	116	45
2	120	45
3	129	49
4	129	64

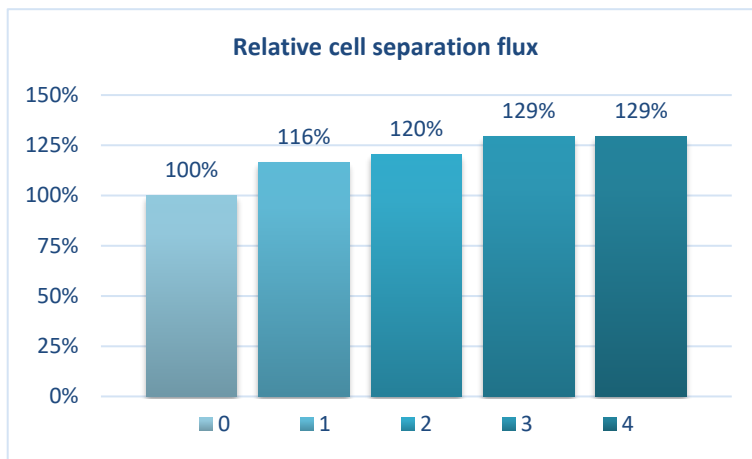


Figure 13. Relative cell separation fluxes for B1.

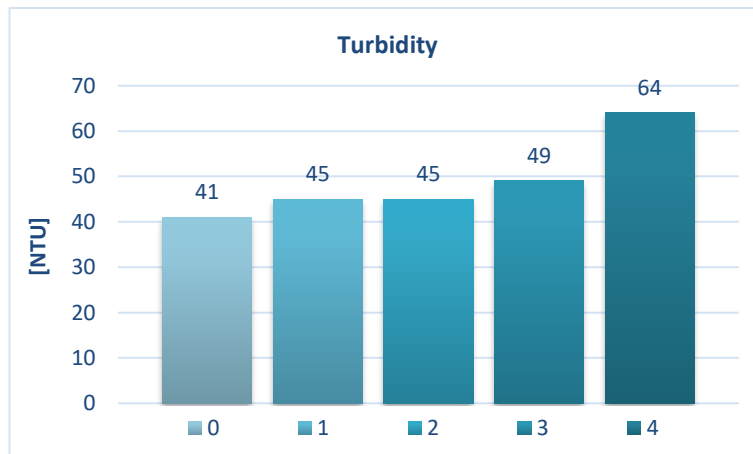


Figure 14. Turbidity of B1 filtrates.

With the most efficient flocculant dosage 3 which had the highest flux and no increase in turbidity, particle count decreased during the rapid mixing phase and was stable during slow mixing phase as seen in Figure 15. With dosage 1 the overall count increased

during rapid mixing and decreased during slow mixing. With the highest dosage the counts of small particles ( $<10\ \mu\text{m}$ ) increased. This can explain the increase in the filtrate turbidity. Dosage 2 gives similar curve compared to dosage 3. Overall, there is only small differences in the chord length distributions and counts before and after flocculation. Rest of the figures can be seen in appendix 1.

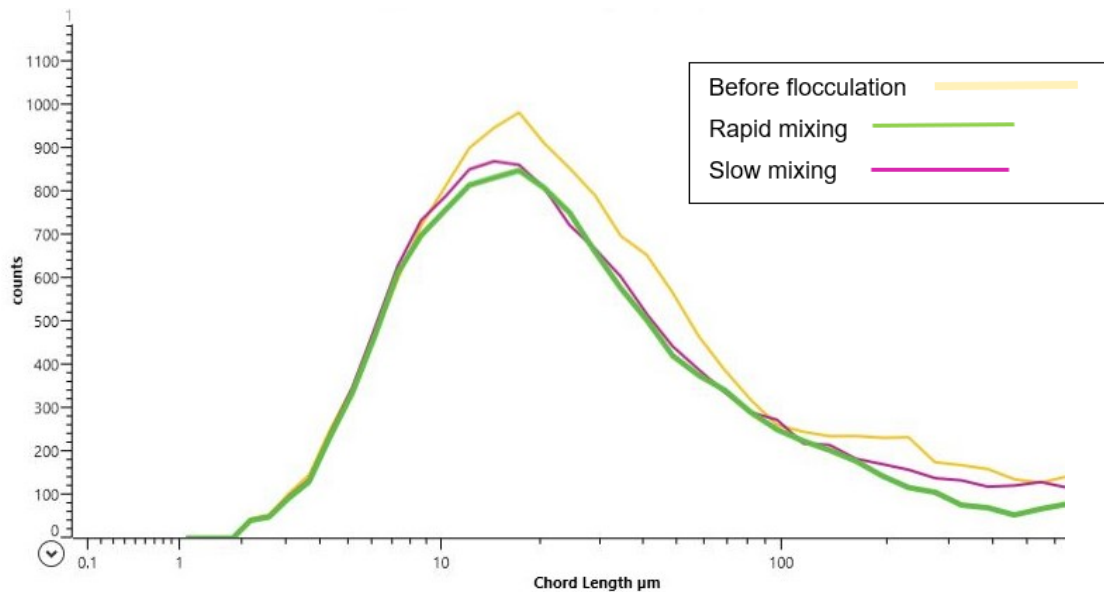


Figure 15. B1 with flocculant dosage 3. Number of counts decreased slightly, and a difference can be seen between rapid and slow mixing phases in particle counts larger than  $100\ \mu\text{m}$ .

Pictures were taken by the Easy Viewer 100 probe. They are very similar to A1 and A2 photos and no difference or visual flocculation can be seen from them.

#### 6.1.4 Optimising flocculation and cell separation of B2

Narrower flocculant amount range was chosen for B2 based on the tests with B1. With B2 the best filtration performance was achieved with dosage 3. The amount of flocculant is the same as in the most efficient one in B1. The numbers in the column Flocculant Dosage are equivalent to the legend of Figure 16 and Figure 17.

Table 8. Filtration data for test series B2.

Flocculation dosage	Relative filtration flux [%]	Filtrate turbidity [NTU]
0	100	47
1	98	46
2	106	47
3	107	49
4	107	52

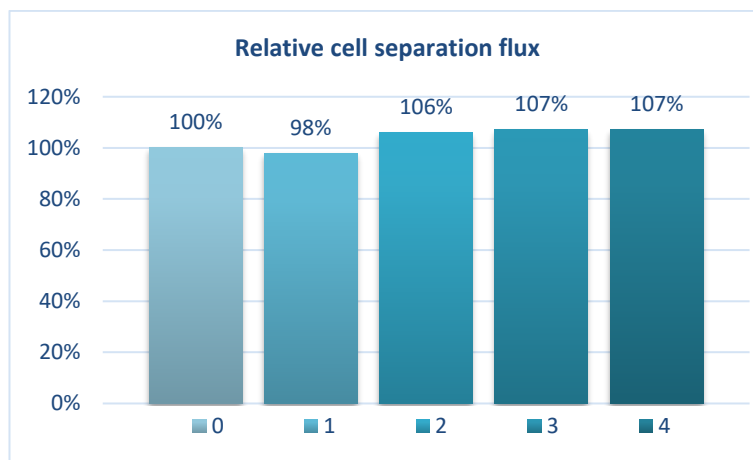


Figure 16. Relative cell separation fluxes for B2.

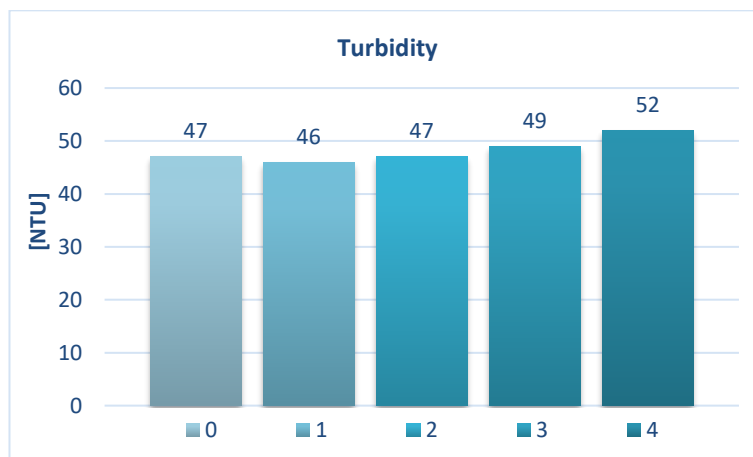


Figure 17. Turbidity of B2 filtrates.

With the most efficient flocculant dosage 3 which had the highest flux and no increase in turbidity particle count decreased during the rapid mixing phase and was stable during slow mixing phase as seen in Figure 18. With dosage 1 and 2 the curves are similar to

dosage 3. With the highest dosage the counts of small particles ( $<10\ \mu\text{m}$ ) increased. This can explain the increase in the filtrate turbidity.

According to the curves there is only relative minor differences in the chord length distributions before and after flocculation. Rest of the figures can be seen in appendix 1.

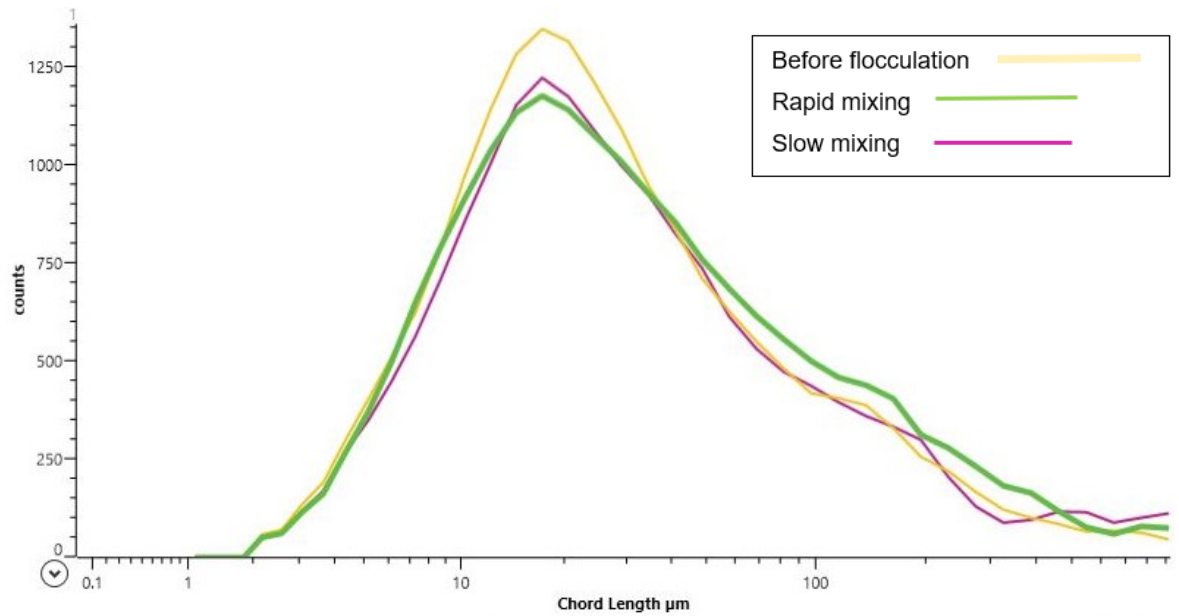


Figure 18. B2 with flocculant dosage 3. Number of counts decreased slightly. Only minor difference can be seen between rapid and slow mixing phases in particle counts in  $>100\ \mu\text{m}$  and  $<10\ \mu\text{m}$ .

Pictures were taken by the Easy Viewer 100 probe. They are very similar to A1, A2 and B1 photos and no difference or visual flocculation can be seen from them.

## 6.2 *Bacillus* processes

### 6.2.1 Optimising flocculation and cell separation of C1

Tests were carried out from two pilot scale fermentations as planned with process C. Coagulation and flocculation were performed with one flocculant agent in four different dosages. Dosages were determined for C2 according to results from C1. Cells were separated from all with Labox25 filter system.

Based on filter data in Table 9 with flocculation dosage 2 the best filtration flux is achieved but higher filtrate quality is achieved with the highest dosage. Compared to filtration without flocculation the flux is 3.8-fold. It is unclear what phenomena is behind this, but

it seems that particles affecting the cell separation are flocculated already with lower flocculant dosage and more particles are forming flocs and filtrated away with higher dosages. The numbers in the column Flocculant Dosage are equivalent to the legend of Figure 19 and Figure 20.

Table 9. Filtration data for test series C1.

Flocculation dosage	Relative filtration flux [%]	Filtrate turbidity [NTU]
0	100	1251
1	330	381
2	375	199
3	346	145
4	262	90

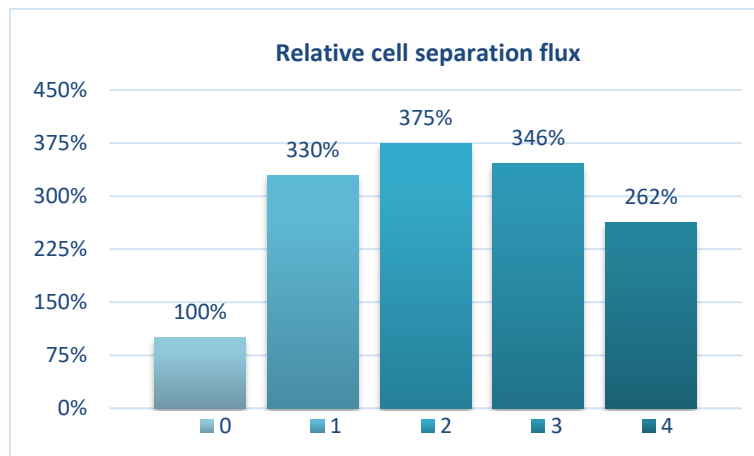


Figure 19. Relative cell separation fluxes for C1.

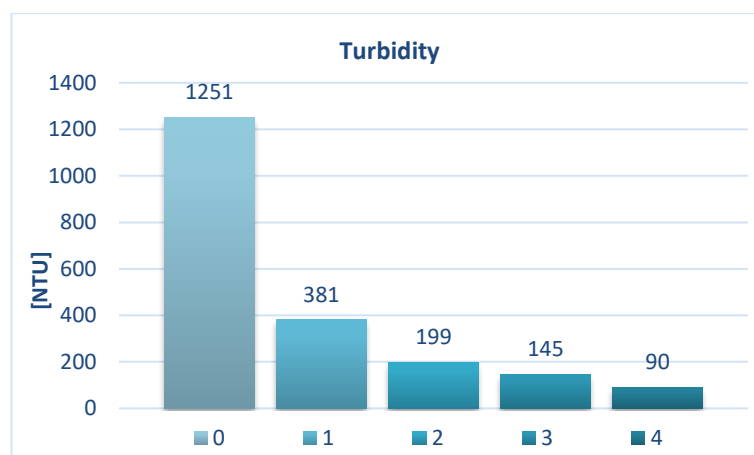


Figure 20. Turbidity of C1 filtrates.

With the most efficient flocculant dosage 2 the count of small particles decreased drastically, and count of large particles increased as it should in flocculation process. There is also clear difference between rapid and slow mixing phase. Count of small particles continued to decrease in slow mixing phase while the number of large particles increased. With every dosage the peak shifted towards larger particles. Curves of dosage 3 in particular were similar to dosage which correlates with the filtration data. All the figures can be seen in appendix 1.

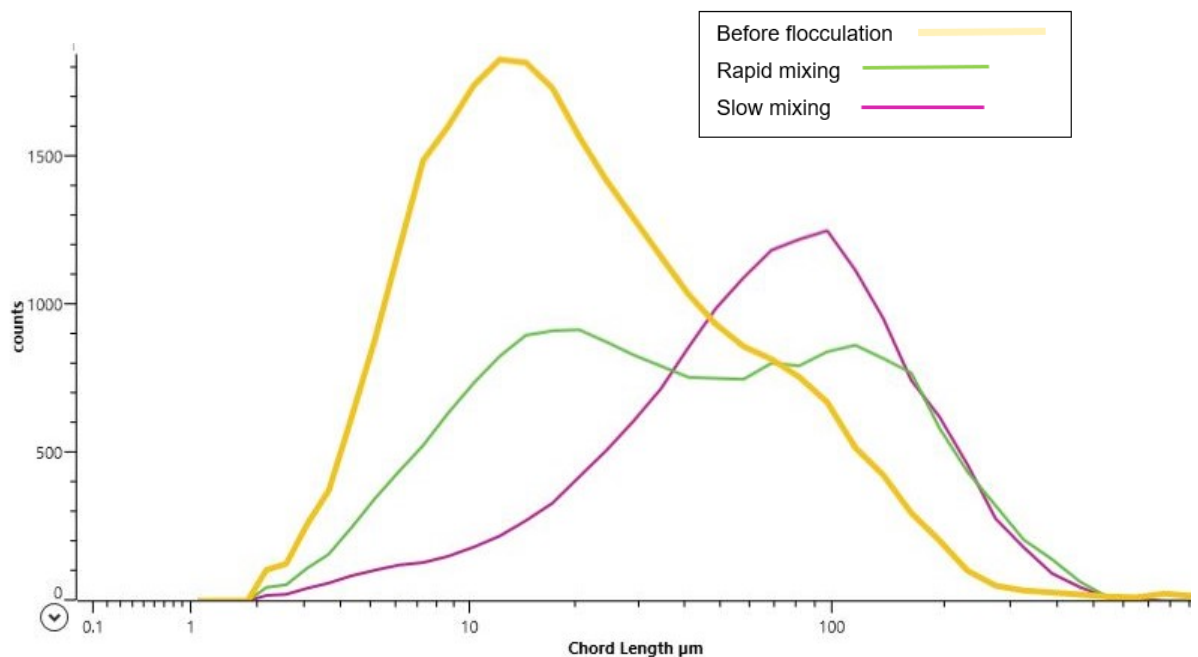
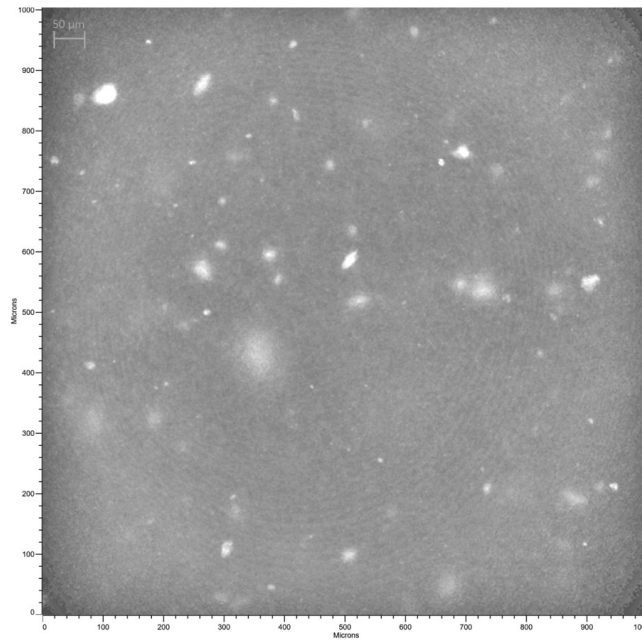


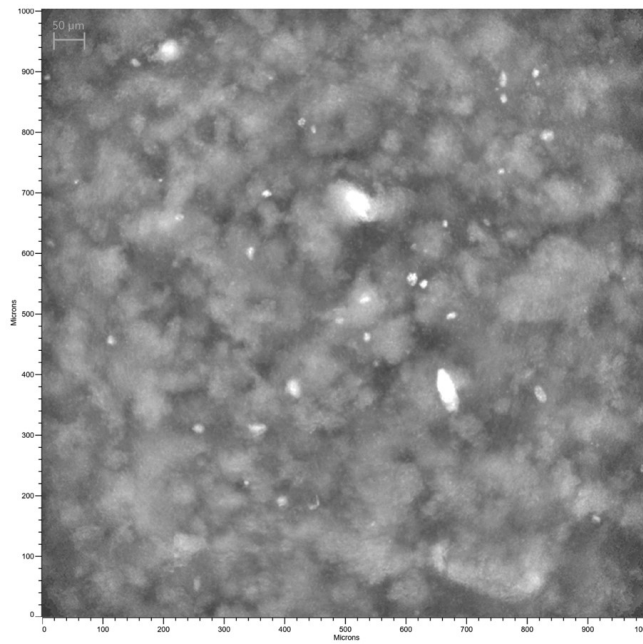
Figure 21. C1 with flocculant dosage 3. The peak shifted towards larger particles after flocculation.

Pictures were taken by the Easy Viewer 100 probe. The pictures differed from the fungi as expected since the cell structure is very different. Floccs are visible to the eye.

From picture 18 halos can be seen in the corners of the capture before the flocculation. The halos are unwanted, and they can distort the results if the system interprets them as very large particles. From figure 21 it can be seen that the system did not interpret the halos as particles since there is no increase in the curves at very large particle. Halos were not visible after flocculation.



Picture 18. Microscopic picture of C1 before flocculation.



Picture 19. C1 after flocculation with dosage 3. The flocs are clearly visible.

### 6.2.2 Optimising flocculation and cell separation of C2

Coagulation and flocculation were performed with one flocculant agent in four different dosages. Dosages were determined for C2 according to results from C1. Cells were separated from all with Labox25 filter system.

Based on filter data in Table 10, with flocculation dosage 2 the best filtration flux is achieved, and filtrate quality is also at rather good level. Compared to filtration without flocculation the flux is 2.5-fold. The numbers in the column Flocculant Dosage are equivalent to the legend of Figure 22 and Figure 23.

Table 10. Filtration data for test series C2.

Flocculation dosage	Relative filtration flux [%]	Filtrate turbidity [NTU]
0	100	980
1	238	72
2	256	80
3	225	81
4	216	72

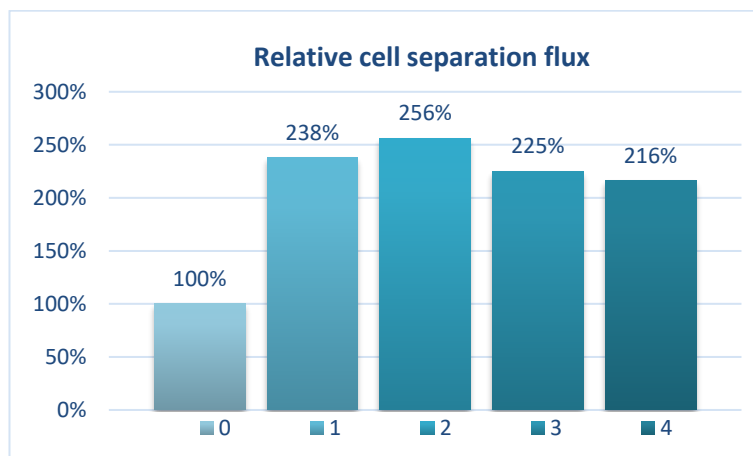


Figure 22. Relative cell separation fluxes for C2.

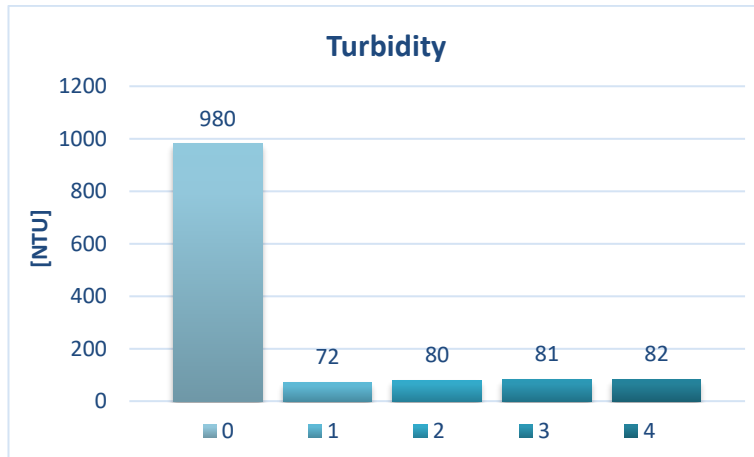


Figure 23. Turbidity of C2 filtrates.

With the most efficient flocculant dosage 2 the count of small particles did not particularly decrease but the number of larger particles increased drastically as seen in Figure 24. It seems that particles which were not visible to the probe aggregated and became visible since the counts went up. There is also clear difference between rapid and slow mixing phase. With every tested dosage, the peak shifted towards larger particles. In particular curves of dosage 1 were similar to the dosage 2 which also correlates with the filtration data. All the figures can be seen in appendix 1.

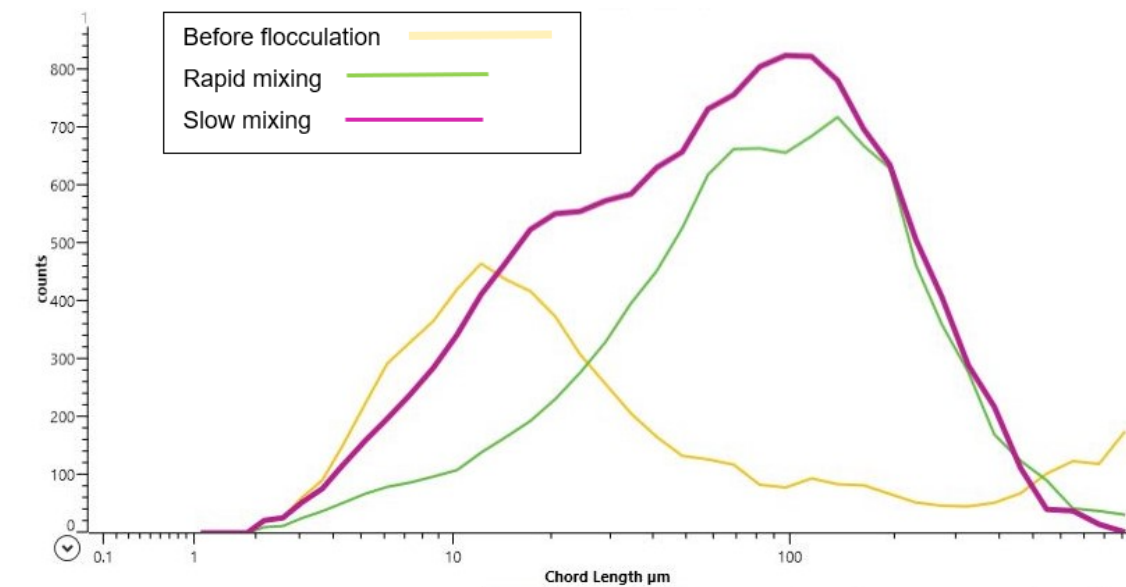
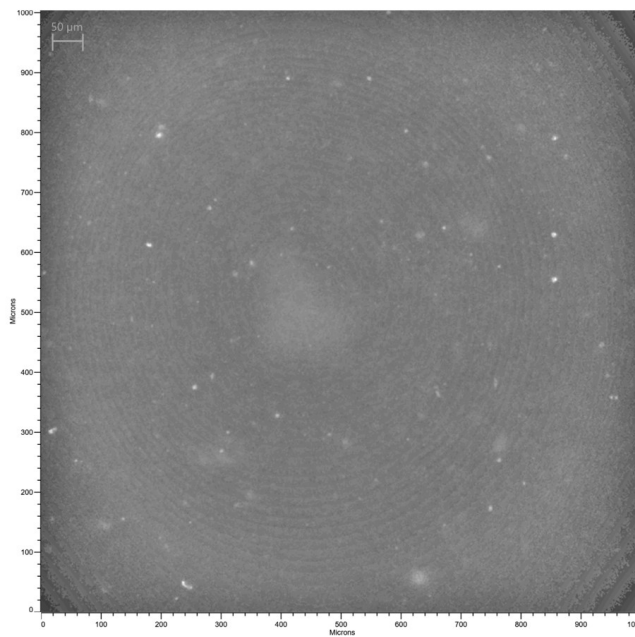


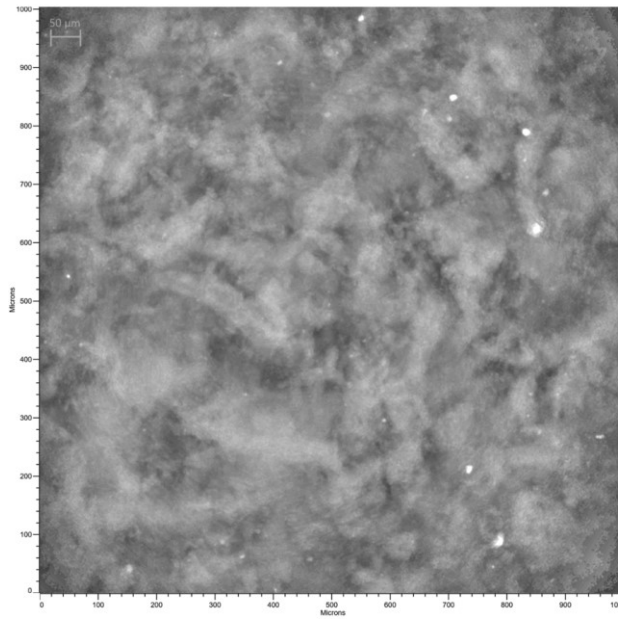
Figure 24. C2 with flocculant dosage 2. The peak shifted towards larger particles after flocculation.

Pictures were taken by the Easy Viewer 100 probe. Compared to C1 the broth contains fewer of the large particles which could be clearly seen as white flakes in Picture 18 of C1. The lack of the larger particles can also be seen from the chord length curve: count of 10  $\mu\text{m}$  particles is at very low level in C2 compared to C1. The flocculation of C2 can also be seen from the Picture 21. It seems that the flocs are rather loosely packed compared to C1, but the most common chord length is the same 100  $\mu\text{m}$ .

From picture 20 it can be seen that there are halos visible in the corners of the capture before the flocculation. The halos are unwanted, and they can distort the results if the system interprets them as very large particles. In Figure 24 the yellow curve increases at the end, and this is most probably caused by the halos since the increase is at very large particles ( $>800 \mu\text{m}$ ). After the flocculation halos were not any more visible and thus did not affect the measurement after the flocculation (Picture 21).



Picture 20. Microscopic picture of C2 before flocculation. Halos are visible in the corners of the picture.



Picture 21. Microscopic picture of C2 after flocculant dosage 2. The flocs are clearly visible.

### 6.2.3 Optimising flocculation and cell separation of D1

Test was carried out from one pilot scale fermentation (D1). Coagulation and flocculation were performed with one flocculant agent in four different dosages.

The best filtration performance was achieved with dosage 1 as seen from Table 11. The turbidity of the filtrate increased significantly with the dosage 1 compared to filtrate without flocculation and with higher flocculant amounts. The numbers in the column Flocculant Dosage are equivalent to the legend of Figure 25 and Figure 26.

Table 11. Filtration data for test series D1.

Flocculation dosage	Relative filtration flux [%]	Filtrate turbidity [NTU]
0	100	930
1	265	230
2	161	550
3	94	700
4	81	850

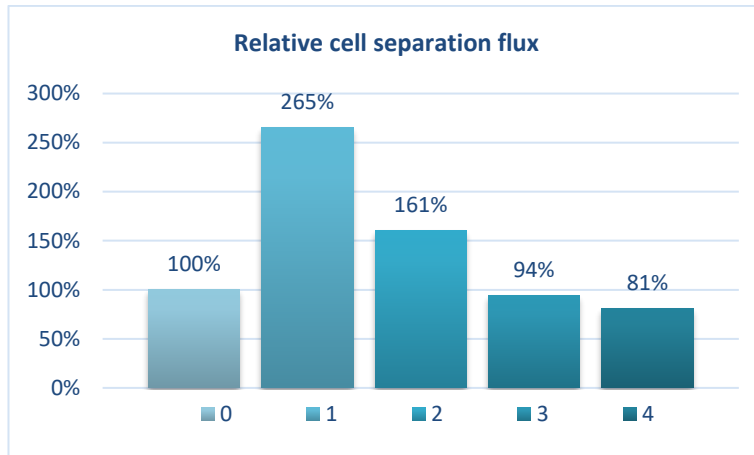


Figure 25. Relative cell separation fluxes for D1.

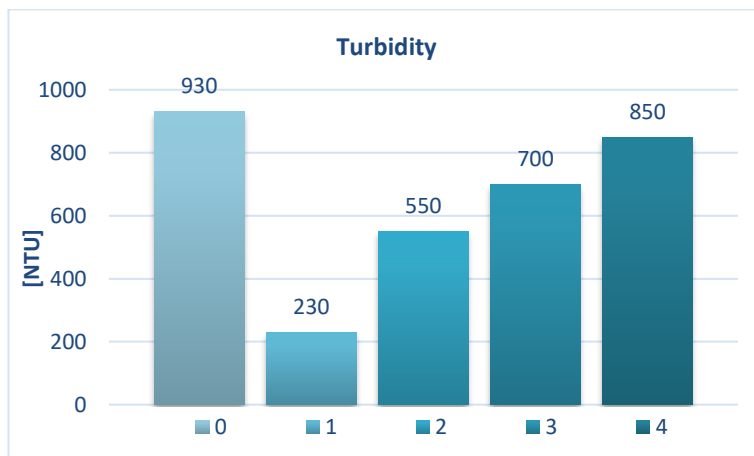


Figure 26. Turbidity of D1 filtrates.

With the most efficient flocculant dosage with the highest flux the count of small particles decreased drastically, and count of large particles increased as it should in flocculation process. Count of small particles continued to decrease in slow mixing phase while the number of large particles increased. With the second lowest dosage there in similar phenomena in particle counts but it is not as drastic. With the two highest dosages the number of particles increased according to the count curves. This might be as a result from overdosing. All the figures can be seen in appendix 1.

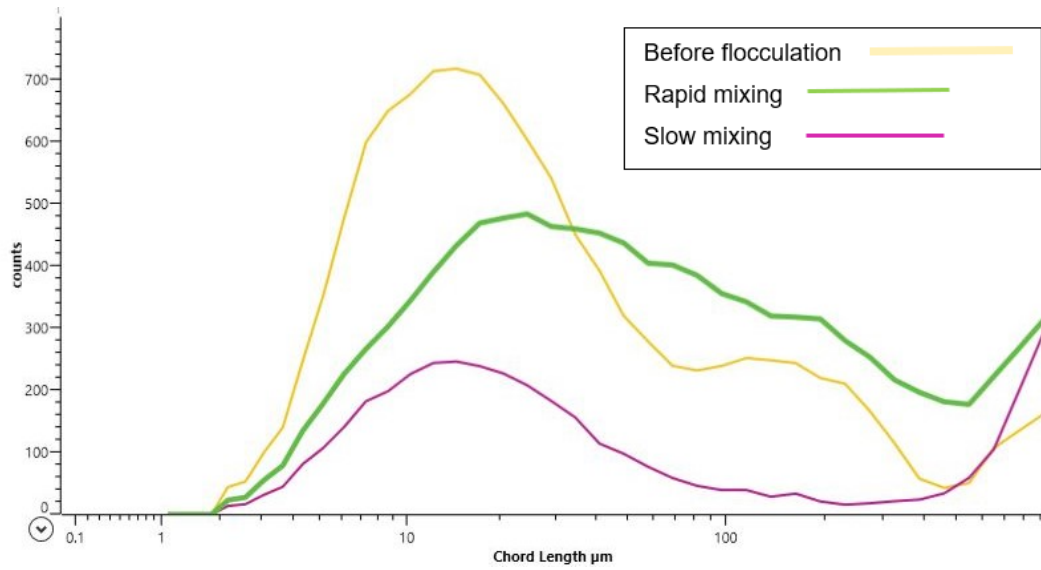
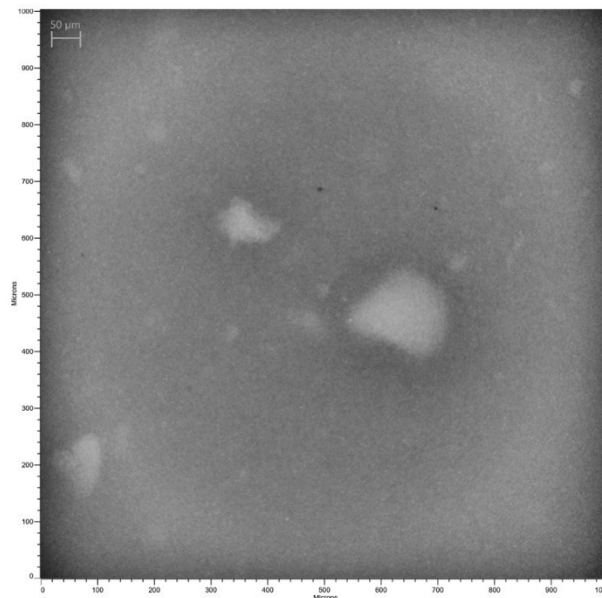
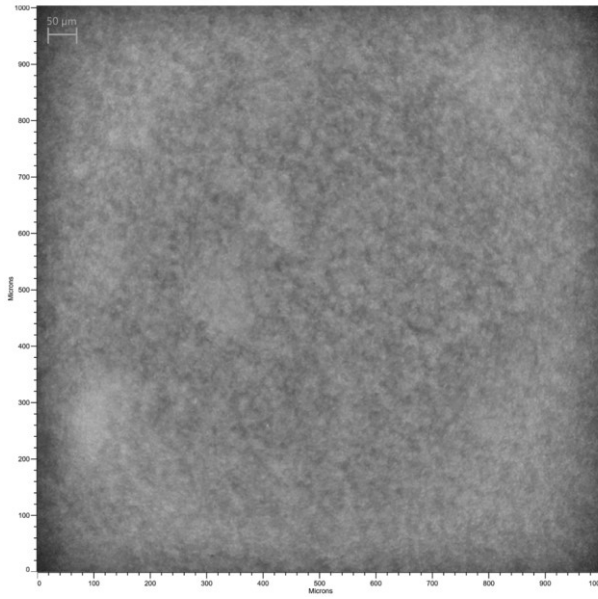


Figure 27. D1 with flocculant dosage 1. Number of small particles decreased, and large ones increased.

The flocculation can also be seen from the microscopic pictures 22 and 23. Particles are clearly packed together after the flocculation but between the different dosages there is no visual difference. Compared process C the flocs are significantly smaller.



Picture 22. Microscopic picture of D1 before flocculation.



Picture 23. Microscopic picture of D1 after flocculation with dosage 1. The flocs are small but still visible to eye.

## 7 CONCLUSIONS

The aim of the thesis was to optimise flocculant amount in two fungal and two *Bacillus* downstream processes using particle vision and measurement -based particle size analysis. Measurements were evaluated with cell separation flux and filtrate quality. Every dosage was first measured with Easy Viewer 100 probe and iC Vision program followed by cell separation with micro scale press filter Labox25 which mimics production scale tower press filter. Filtrate quality was based on turbidity measurements. The lower the turbidity the higher the quality.

Optimal flocculant amount was found for both fungal broths A and B. Despite cultivations being laboratory and pilot scale, the best flocculant amount was the same in both scales. Based on the results it can be concluded that there is no upscaling effect which could affect the flocculation. Overall, the differences were minor and difficult to interpret in the chord length distributions. There was also no change in the microscopic pictures before and after flocculation and thus filtration data is needed to support the chord length curves. After flocculation total amount of particles should decrease and the peak of the curve should shift towards the larger particles. This did not happen with the fungal processes.

With *Bacillus* processes the results were promising. Clear shift in the chord length distribution was seen and there were clear differences between the dosages. Flocculation could also be observed from the pictures taken by the probe. With process C, the optimal flocculant amount was able to be defined. Filtration fluxes and the particle size distribution correlated well. Only the difference between the two best dosages is difficult to observe from the particle size curves. The difference is very clear for the other dosages in filtration fluxes but also in the curves.

For process D, only one test was carried out. The curves differed significantly between the different dosages. With the optimal amount based on the filtration flux the number of small particles decreased drastically and number of very large particles spiked. This was the smallest tested amount and thus the dosage should be confirmed by narrower and more optimal dosage range.

When comparing fungal and *Bacillus* results there is correlation between the filtration fluxes, pictures, and particles' size distribution. In fungal tests only minor shifts were seen in the particle size curves, no changes were seen in the pictures and there was only

minor increase in the cell separation flux when compared with the flux without flocculation. The flocculation did increase the filtrate quality when dosed the optimal amount. With *Bacillus* there was a clear shift in particle distribution towards larger particles, flocs were visible to the eye and the fluxes multiplied in comparison with flux without flocculation. The difference results from different cell structure and culture media.

The Easy Viewer 100 was used for the first time for this purpose. As the work progressed the technique became more familiar, and the tests were faster to conduct. Learning curve was steep at the beginning but more effort could have been put to getting more familiar with the analysis tools of iC Vision but due to time limitations this was not done.

Technical difficulties with the Easy Viewer 100 probe caused unreliability to the results. For unknown reason circles or halos appeared in some pictures and this could have disturbed the particle size analysis since it is based on the pictures. For instance, in dosage 1 of B1 the halo on the outer edges caused a spike in the large particles and the number of smaller particles is less than in the other dosages. The halos were the strongest with C2. Work is underway with the equipment manufacturer to get clarity to the issue.

Fungal broths are known to be challenging for many probes and imaging tools due to cell structure and cell density. Therefore, the result was somewhat expected despite promising results in the feasibility study conducted earlier with FBRM. Only small changes can be seen after the flocculation in particle size curves. These were rather difficult to observe also in the picture, so it is highly important to use the correct picture for the analysis. Many of the pictures were out of focus due to the high density and therefore should not be used for the analysis. For both the fungal and *Bacillus* broths it is extremely important to conduct the measurement in the similar way.

There was limited amount of *Bacillus* materials available in the time window of the thesis. This caused some limitations and increased the unreliability of the results. Between process C and D there was significant difference in the chord length curves which could be confirmed with more tests. The strain background in the processes are different and could explain the differences. Despite the small amount of *Bacillus* tests, particle vision and measurement-based particle size analysis could be used with *Bacillus* broths, but more data should be gathered to be able to rely solely on the particle size analysis. Until there is sufficient amount of data, filtration test should be carried out alongside the particle size analysis. Work will continue on this also after the thesis.

For fungal broths, FBRM based particle size analysis could be tested as an option and continue with cell separation tests for accurate flocculant dosing.

The importance of the coagulation-flocculation process can be clearly seen in the filtration data. With *Bacillus* broths the filtration fluxes were increased with optimal dosage by 2.5 – 4-fold compared to flux without flocculation and the qualities improved significantly. In production such a difference in flux could mean days difference in filtration duration. With fungal broths the differences were not as significant but still considerable when there are production size batches to be filtrated.

## REFERENCES

- Ali, E., Muyibi, S., Salleh, H., Salleh, M. & Alam, Z. (2009) Moringa Oleifera seed as natural coagulant for water treatment. Thirteenth International Water Technology Conference. [https://www.researchgate.net/publication/242313845\\_MORINGA\\_OLEIFERA\\_SEEDS\\_AS\\_NATURAL\\_COAGULANT\\_FOR\\_WATER\\_TREATMENT](https://www.researchgate.net/publication/242313845_MORINGA_OLEIFERA_SEEDS_AS_NATURAL_COAGULANT_FOR_WATER_TREATMENT). Retrieved 29.1.2022.
- Ajao, V., Fokkink, R., Leermakers, F., Bruning, H., Rijnaarts, H., & Temmink, H. (2020). Bio flocculants from wastewater: Insights into adsorption affinity, flocculation mechanisms and mixed particle flocculation based on biopolymer size-fractionation. *Journal of Colloid and Interface Science*, 581, 533-544. <https://doi-org.ezproxy.turkuamk.fi/10.1016/j.jcis.2020.07.146>
- Aldajani, M., Alipoormazandarani, N., Kong, F., & Fatehi, P. (2021). Acid hydrolysis of kraft lignin-acrylamide polymer to improve its flocculation affinity. *Separation and Purification Technology*, 258, 117964. <https://doi-org.ezproxy.turkuamk.fi/10.1016/j.seppur.2020.117964>.
- Bratby, J. (2016). *Coagulation and flocculation in water and wastewater treatment (Third edition)*. IWA Publishing.
- Chianese, A. & Kramer, H. J. M. (2012). *Industrial crystallization process monitoring and control*. Wiley-VCH.
- Dayarathne, H. N. P., Angove, M. J., Aryal, R., Abuel-Naga, H., & Mainali, B. (2021). Removal of natural organic matter from source water: Review on coagulants, dual coagulation, alternative coagulants, and mechanisms. *Journal of Water Process Engineering*, 40, 101820. <https://doi-org.ezproxy.turkuamk.fi/10.1016/j.jwpe.2020.101820>.
- Esmaeilnejad-Ahranjani, P., & Hajimoradi, M. (2022). Optimization of industrial-scale centrifugal separation of biological products: comparing the performance of tubular and disc stack centrifuges. *Biochemical Engineering Journal*, 178, 108281. <https://doi-org.ezproxy.turkuamk.fi/10.1016/j.bej.2021.108281>
- Evans, M. (2003). *Optimisation of manufacturing processes: A response surface approach*. Maney for the Institute of Materials, Minerals and Mining.
- Flickinger M. C., *Downstream Industrial Biotechnology: Recovery and Purification* (2013). John Wiley & Sons, Incorporated.
- Hadiyanto, H., Christwardana, M., Widayat, W., Jati, A. K., & Laes, S. I. (2021). Optimization of flocculation efficiency and settling time using chitosan and eggshell as bio-flocculant in *Chlorella pyrenoidosa* harvesting process. *Environmental Technology & Innovation*, 24, 101959. <https://doi-org.ezproxy.turkuamk.fi/10.1016/j.eti.2021.101959>
- Harrison, R. G., Todd, P. W., Rudge, S. R., & Petrides, D. P. (2015). *Bioseparations Science and Engineering*. Oxford University Press, Incorporated.
- Kemira Oyj. (2021). *Superfloc Flocculants & Coagulants [Brochure]*. <http://www.greensound.fi/i3/greenmining/attachments/kemira/kemira3.pdf>. Retrieved April 11, 2021.
- Kyoda, Y., Costine, A. D., Fawell, P. D., Bellwood, J., & Das, G. K. (2019). Using focused beam reflectance measurement (FBRM) to monitor aggregate structures formed in flocculated clay suspensions. *Minerals Engineering*, 138, 148-160. <https://doi-org.ezproxy.turkuamk.fi/10.1016/j.mineng.2019.04.045>

Liow Y-T. (1991). A contour tracing algorithm that preserves common boundaries between regions. *CVGIP: Image Understanding*, 53(3), 313–321. [https://doi.org/10.1016/1049-9660\(91\)90019-L](https://doi.org/10.1016/1049-9660(91)90019-L).

Liu, T., He, Z., Hu, H., & Ni, Y. (2011). Treatment of APMP pulping effluent based on aerobic fermentation with *Aspergillus niger* and post-coagulation/flocculation. *Bioresource Technology*, 102(7), 4712-4717. <https://doi-org.ezproxy.turkuamk.fi/10.1016/j.biortech.2011.01.047>

Mettler-Toledo. (2021). Analyzer Easy Viewer 100 System. [https://www.mt.com/sg/en/home/products/L1\\_AutochemProducts/FBRM-PVM-Particle-System-Characterization/easyviewer/easyviewer-100.html](https://www.mt.com/sg/en/home/products/L1_AutochemProducts/FBRM-PVM-Particle-System-Characterization/easyviewer/easyviewer-100.html). Retrieved April 10, 2021.

Mettler-Toledo. (2021). Flocculation – Develop a flocculation process with control of the particle distribution. [https://www.mt.com/de/en/home/applications/L1\\_AutoChem\\_Applications/L2\\_ParticleProcessing/Formulation\\_Flocculation.html](https://www.mt.com/de/en/home/applications/L1_AutoChem_Applications/L2_ParticleProcessing/Formulation_Flocculation.html). Retrieved April 10, 2021

Mortadia, A., Chahida, E. G., Elmelouky, A., Chahbia, M., Ghyatia, N. EL., Zaima, S., O.Cherkaouib Mozninea, R. El. (2020). Complex electrical conductivity as a new technique to monitor the coagulation-flocculation processes in the wastewater treatment of the textile Industry. *Water Resources and Industry*, 24, 100130. <https://doi.org/10.1016/j.wri.2020.100130>.

Nazemzadeh, N., Malanca, A. A., Nielsen, R. F., Gernaey, K. V., Andersson, M. P., & Mansouri, S. S. (2021). Integration of first-principle models and machine learning in a modeling framework: An application to flocculation. *Chemical Engineering Science*, 245, 116864. <https://doi-org.ezproxy.turkuamk.fi/10.1016/j.ces.2021.116864>

Pandey, A. (2014). *Biofuels from algae* (First edition ed.). Elsevier.

Perlmutter, B. (2015). *Solid-Liquid Filtration: Practical Guides in Chemical Engineering*. Elsevier Science & Technology.

Ramos, J. J., Leiva, W. H., Castillo, C. N., Ihle, C. F., Fawell, P. D., & Jeldres, R. I. (2020). Seawater flocculation of clay-based mining tailings: Impact of calcium and magnesium precipitation. *Minerals Engineering*, 154, 106417. <https://doi-org.ezproxy.turkuamk.fi/10.1016/j.mineng.2020.106417>

Sarasti, J. (2017). Suitability of candle filter for enzyme solution clarification and microbiological purification. Aalto University School of Chemical Engineering.

Sankaranarayanan, S., Likozar, B. & Navia, R. (2019). Real-time Particle Size Analysis Using the Focused Beam Reflectance Measurement Probe for In Situ Fabrication of Polyacrylamide–Filler Composite Materials. *Sci Rep* 9, 10126. <https://doi.org/10.1038/s41598-019-46451-x>.

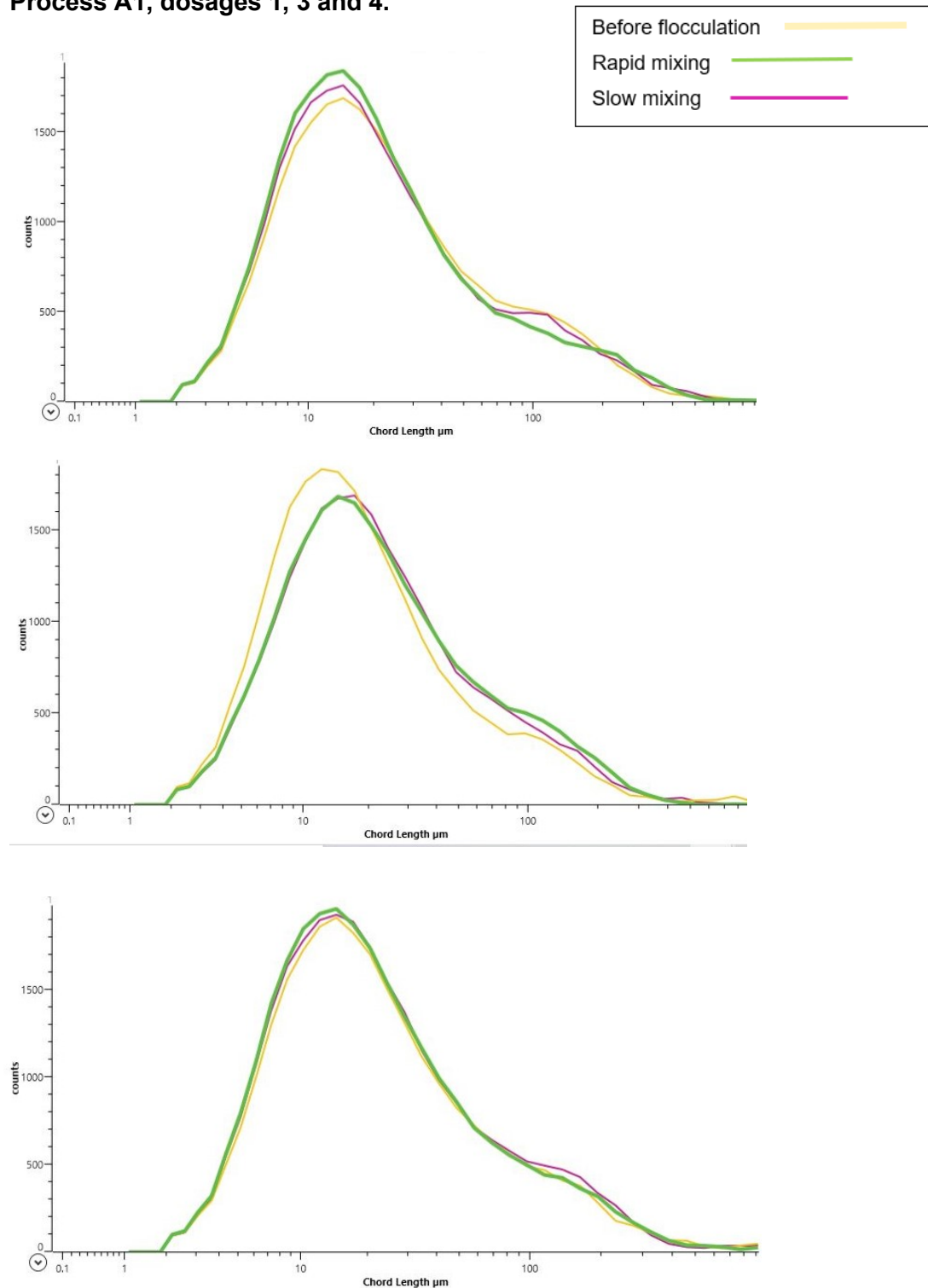
Sustainable Sanitation and Water Management (SSWM). (2021). Coagulation-Flocculation. <https://sswm.info/sswm-university-course/module-6-disaster-situations-planning-and-preparedness/further-resources-0/coagulation-flocculation>. Retrieved April 10, 2021.

Tadros, T. F. (2017). *Basic Principles of Interface Science and Colloid Stability*. Walter de Gruyter GmbH.

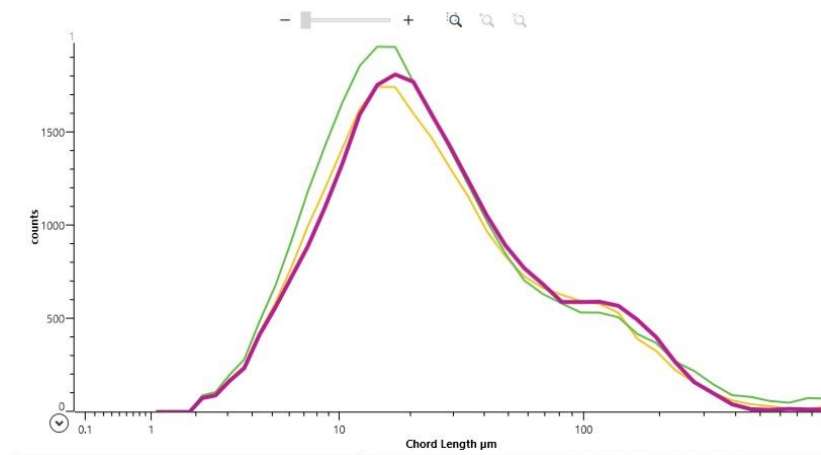
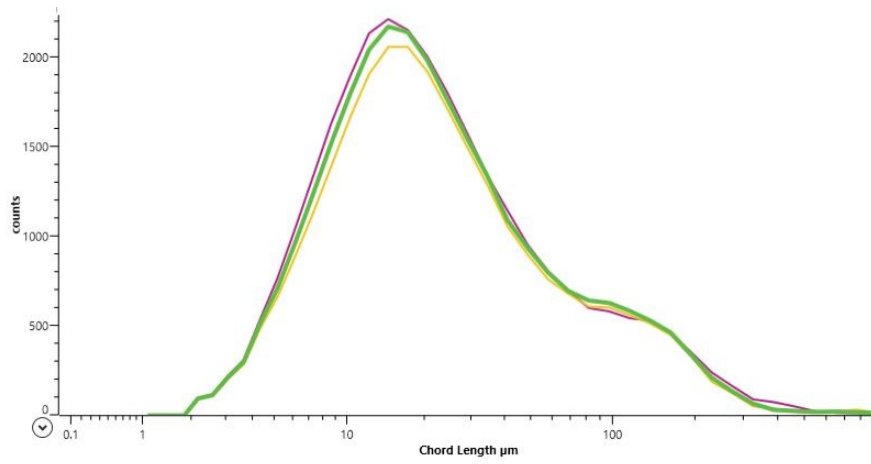
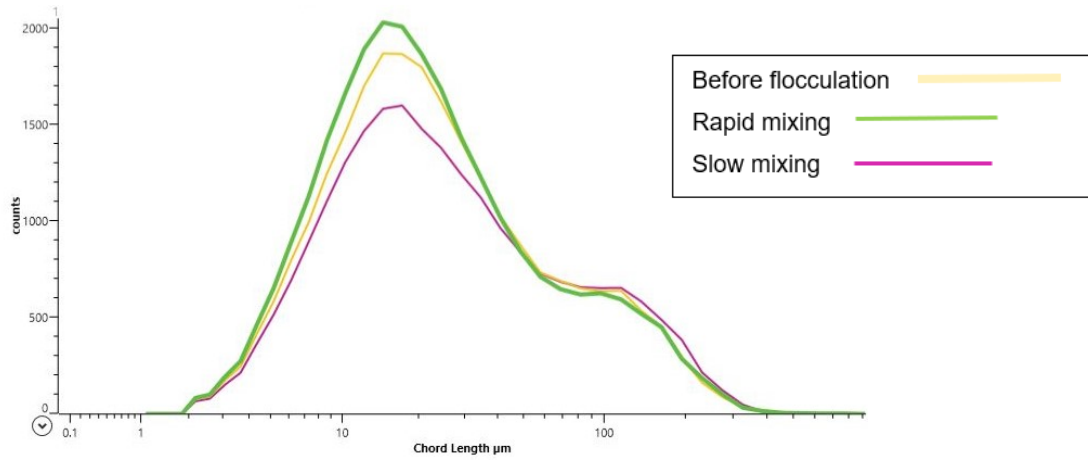
Todaro C. C. & Vogel H. C., *Fermentation and Biochemical Engineering Handbook* (2014). Elsevier Science & Technology Books.

## Chord length distributions for every flocculant dosage

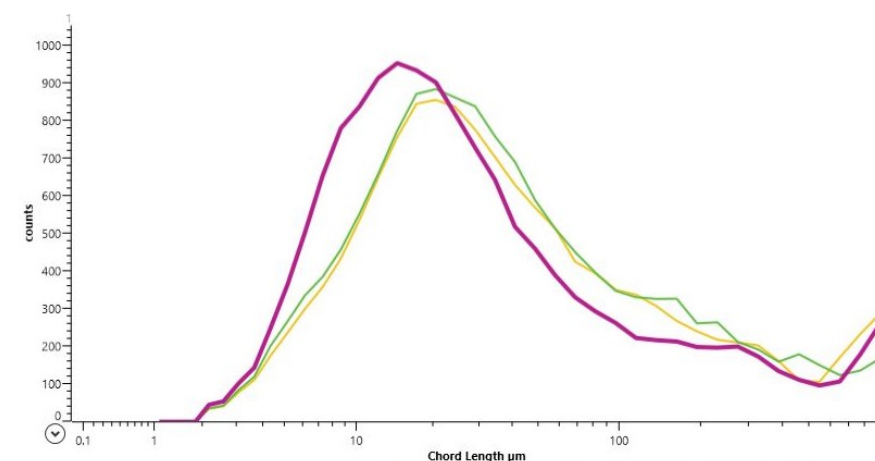
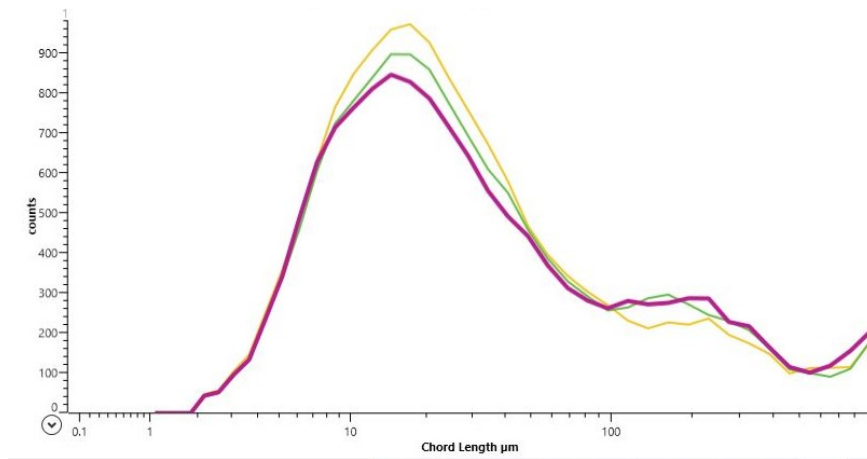
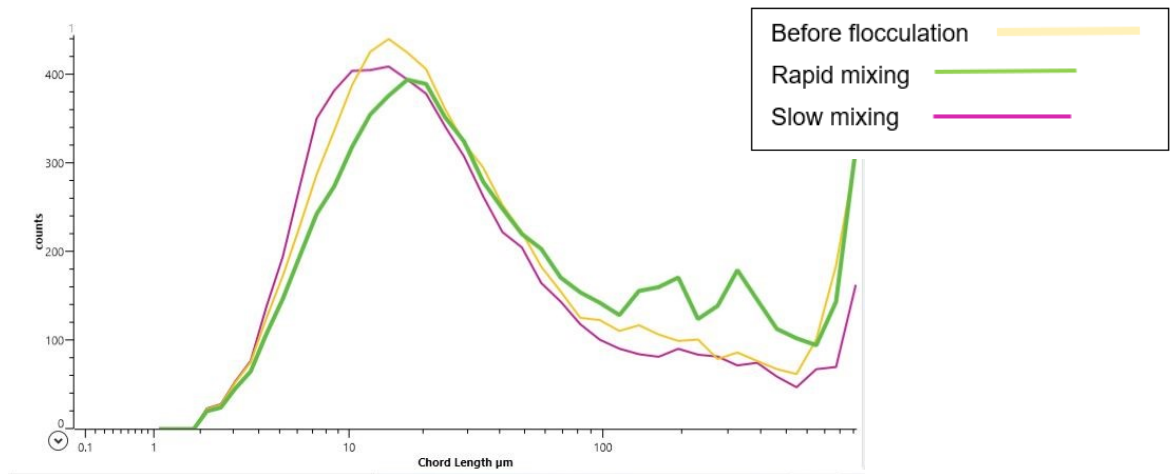
Process A1, dosages 1, 3 and 4.



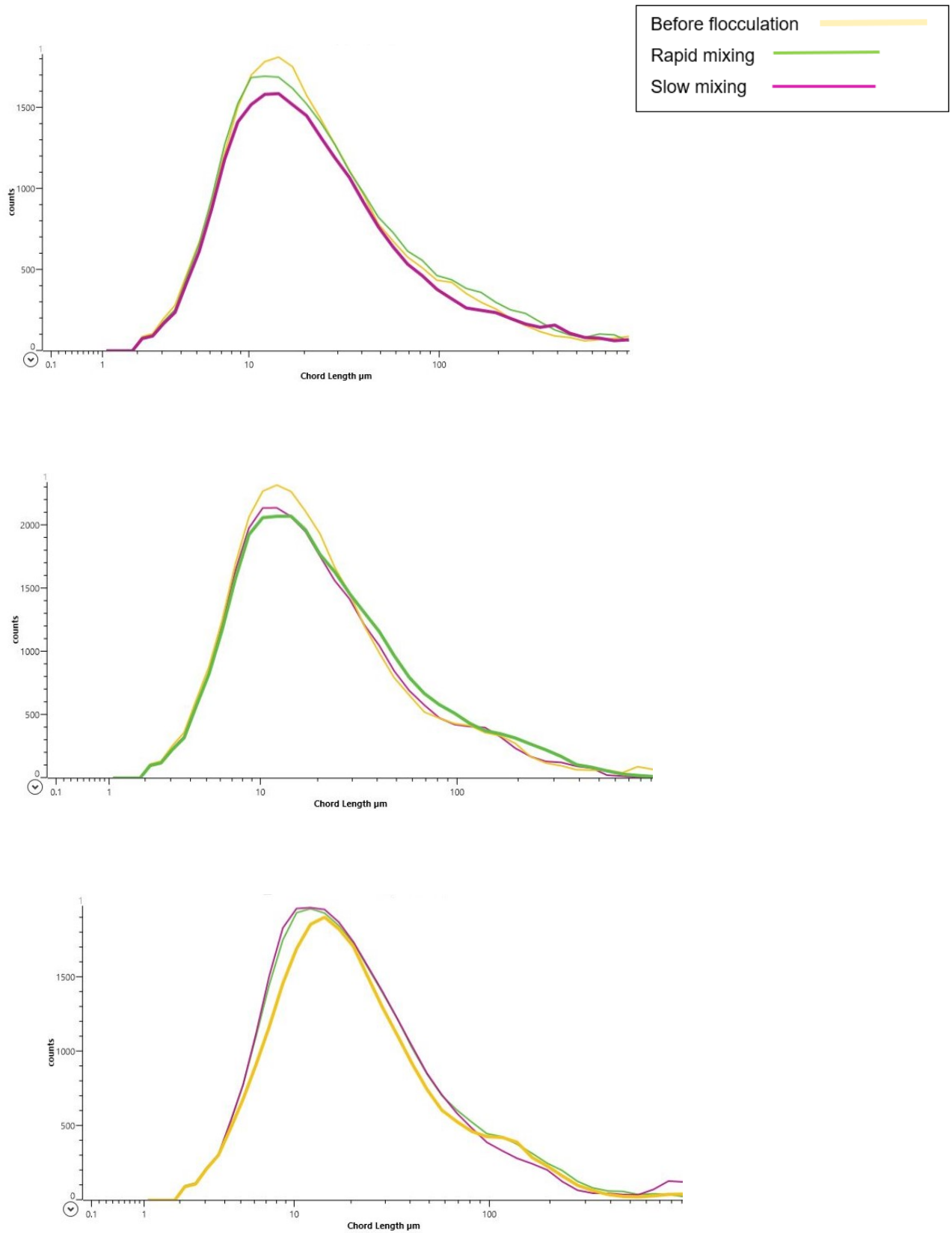
Process A2, dosages 1, 2 and 4.



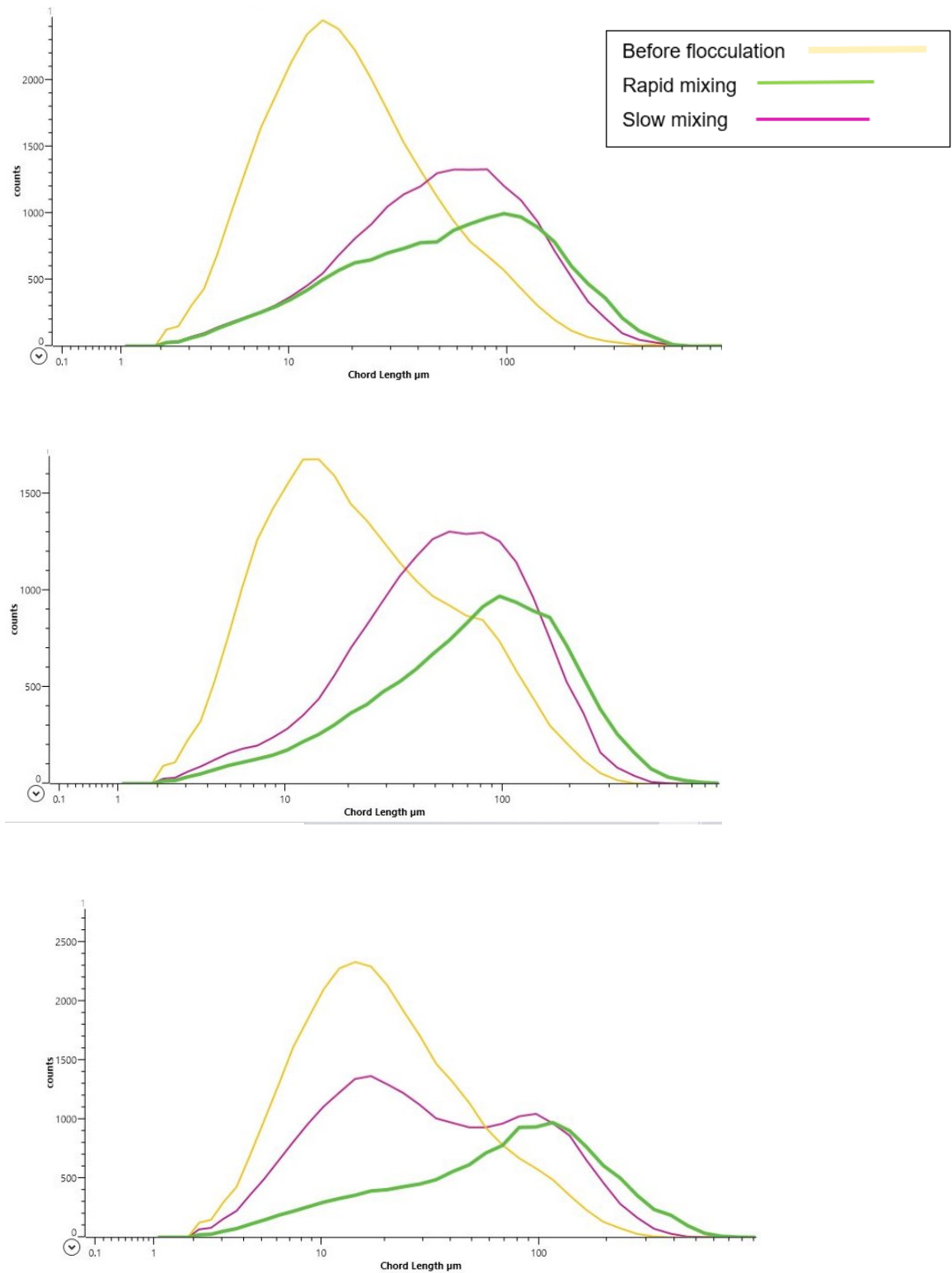
Process B1, dosages 1, 2 and 4



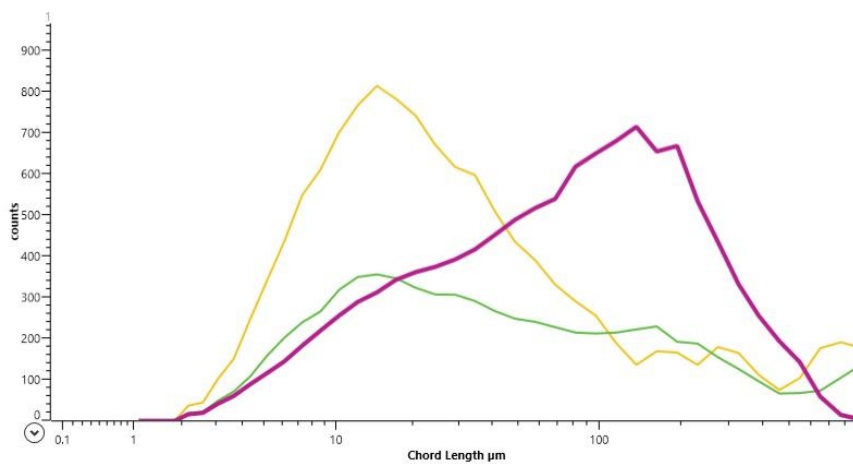
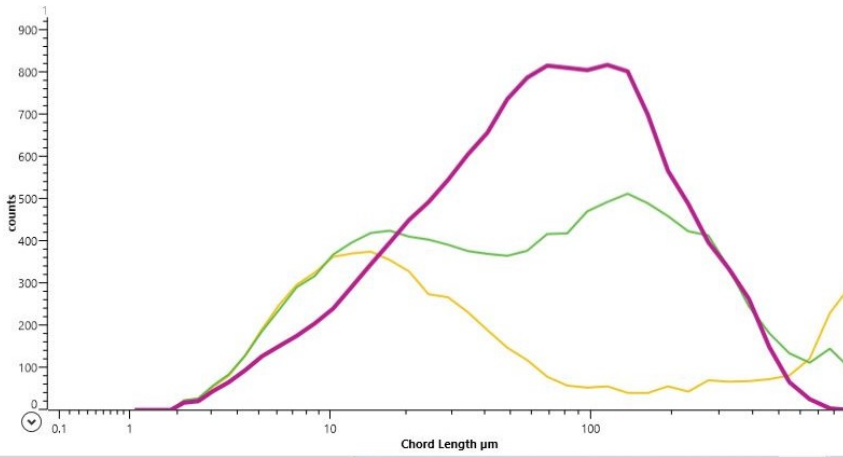
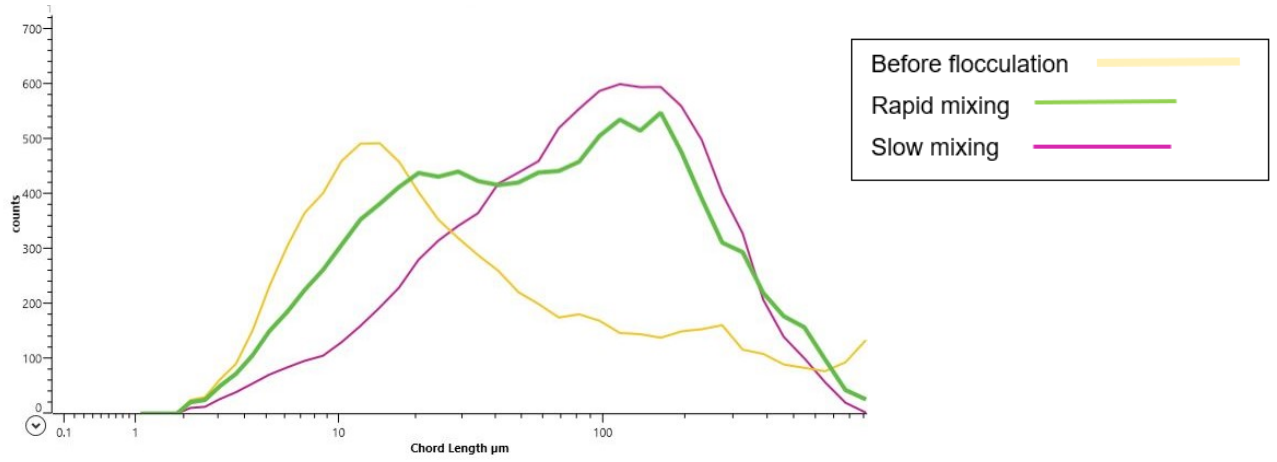
## Process B2, dosages 1, 2 and 4



## Process C1, dosages 1, 3 and 4



Process C2, dosages 1, 3 and 4



Process D1, dosages 2, 3 and 4

